DISSERTATIONES
CHIMICAE
UNIVERSITATIS
TARTUENSIS
235

SILVESTER JÜRJO

Separation of rare earth elements from Estonian phosphorite ore using liquid extraction followed by electrochemical reduction

DISSERTATIONES CHIMICAE UNIVERSITATIS TARTUENSIS
235

DISSERTATIONES CHIMICAE UNIVERSITATIS TARTUENSIS
235

SILVESTER JÜRJO

Separation of rare earth elements from Estonian phosphorite ore using liquid extraction followed by electrochemical reduction

UNIVERSITY OF TARTU
Press
1632

Institute of Chemistry, Faculty of Science and Technology, University of Tartu, Estonia

The dissertation was accepted for the commencement of the degree of Doctor of Philosophy in Chemistry on October 28th, 2024, by the Council of Institute of Chemistry, University of Tartu.

Supervisors: Professor Enn Lust, PhD
University of Tartu, Estonia

Research Ove Oll, PhD
University of Tartu, Estonia

Opponent: Prof. Dr. Pawel J. Kulesza, University of Warsaw, Poland

Commencement: December 20th, 2024 at 10.15, Ravila 14A-1020, Tartu (Chemicum) and Microsoft Teams

This research was funded by the Estonian Ministry of Education and Research (projects no. PRG676, PSG249), the Education and Youth Board projects ÕÜF12 and ÕÜF13, and by the EU through the European Regional Development Fund Centers of Excellence, TK210 (01.01.2024–31.12.2030).

ISSN 1406-0299 (print)
ISBN 978-9916-27-727-0 (print)
ISSN 2806-2159 (pdf)
ISBN 978-9916-27-728-7 (pdf)

University of Tartu Press
www.tyk.ee

TABLE OF CONTENTS

1. LIST OF ORIGINAL PUBLICATIONS 7

2. ABBREVIATIONS AND SYMBOLS 8

3. INTRODUCTION 9

4. LITERATURE OVERVIEW 10
   4.1. Rare earth elements 10
   4.2. Ionic liquids 11
   4.3. Processing methods for rare earth elements 12
      4.3.1. Hydrometallurgical route 12
      4.3.2. Electrochemical route 13
   4.4. Electrochemical characterization techniques 14
      4.4.1. Cyclic voltammetry 14
      4.4.2. Constant potential technique 14
      4.4.3. Electrochemical impedance spectroscopy 15
   4.5. Microscopic and spectroscopic characterization techniques 17
      4.5.1. Inductively coupled plasma mass spectroscopy (ICP-MS) and microwave plasma atomic emission spectroscopy (ICP-AES) . 17
      4.5.2. XRD and XRF methods 17

5. EXPERIMENTAL 18
   5.1. Liquid extraction 19
      5.1.1. Raw materials and chemicals in liquid extraction experiments .. 19
      5.1.2. Modification of Aliquat 336 with 2.5 M KNO_3 19
      5.1.3. Feed solutions in liquid extraction experiments 19
      5.1.4. Equipment 20
      5.1.5. Experimental conditions 20
   5.2. Electrochemical separation 22
      5.2.1. First set of experiments – electrochemical separation of praseodymium from praseodymium trinitrate salt 22
      5.2.2. Second set of experiments – electrochemical separation of yttrium from other REEs using phosphorite ore as the starting material 23
   5.3. Microscopic and spectroscopic analysis 24

6. RESULTS AND DISCUSSION 25
   6.1. Liquid extraction 25
      6.1.1. First extraction step for U, Th, and Tl removal from concentrated nitric acid media 25
      6.1.2. Extraction of REEs from Partially Neutralized Nitric Acid Media 25
      6.1.3. Extraction of REEs from 3M hydrochloric acid media 27
      6.1.4. Extraction of other elements than REE from 3M hydrochloric acid media 29

6.2. Electrochemical separation 29
6.2.1. Electrochemical separation of praseodymium from praseodymium trinitrate salt solution 29
6.2.2. Electrochemical separation of yttrium from phosphorite ore 33
7. SUMMARY 39
8. REFERENCES 40
9. SUMMARY IN ESTONIAN 48
10. ACKNOWLEDGEMENTS 50
11. PUBLICATIONS 51
CURRICULUM VITAE 86
ELULOOKIRJELDUS 87

1. LIST OF ORIGINAL PUBLICATIONS

I Jürjo, Silvester; Siinor, Liis; Siimenson, Carolin; Paiste, Päärn; Lust, Enn. Two-Step Solvent Extraction of Radioactive Elements and Rare Earths from Estonian Phosphorite Ore Using Nitrated Aliquat 336 and Bis(2-ethylhexyl) Phosphate. Minerals 2021, 11 (4), 388

II Jürjo, Silvester; Oll, Ove; Paiste, Päärn; Külaviir, Marian; Zhao, Jinfeng; Lust, Enn. Electrochemical co-reduction of praseodymium and bismuth from 1-butyl-1-methylpyrrolidinium bis(fluorosulfonyl)imide ionic liquid. Electrochemistry Communications 2022, 138, 107285

III Jürjo, Silvester; Oll, Ove; Lust, Enn. Yttrium Separation from Phosphorite Extract Using Liquid Extraction with Room Temperature Ionic Liquids Followed by Electrochemical Reduction. Metals 2024, 14, 927

Author's contribution:

Paper I: Investigation, Methodology, Writing – original draft.

Paper II: Investigation, Methodology, Writing – original draft.

Paper III: Paper II: Investigation, Methodology, Writing – original draft.

2. ABBREVIATIONS AND SYMBOLS

AC	–	alternating current
AES	–	atomic emission spectroscopy
$Bi(OTf)_3$	–	bismuth(III) trifluoromethanesulfonate
BMPyrrFSI	–	1-Butyl-1-methylpyrrolidinium bis(fluorosulfonyl)imide
C_O	–	concentration of oxidized form
C_P	–	parallel differential capacitance
C_R	–	concentration of reduced form
C_S	–	series differential capacitance
CV	–	cyclic voltammetry
DC	–	direct current
D2EHPA	–	bis(2-ethylhexyl) phosphate
DFT	–	density functional theory
EC	–	equivalent circuit
EDS	–	energy dispersive X-ray spectroscopy
EIS	–	electrochemical impedance spectroscopy
HREE	–	heavy rare earth elements
ICP-MS	–	Inductively Coupled Plasma Mass Spectrometry
i	–	electrode current
IL	–	ionic liquid
j	–	electrode current density
k_0	–	standard heterogeneous rate constant
k_b	–	heterogeneous rate constant for oxidation
k_f	–	heterogeneous rate constant for reduction
LREE	–	light rare earth elements
MP-AES	–	Microwave plasma atomic emission spectroscopy
O	–	oxidized form of the standard system
R	–	reduced form of the standard system
REE	–	rare earth elements
RTIL	–	room temperature ionic liquid
SEM	–	scanning electron microscopy
TFSI	–	bis-trifluoromethylsulfonylimide
Z	–	impedance
Z'	–	real part of impedance
Z''	–	imaginary part of impedance

3. INTRODUCTION

Rare earth elements (REEs) are strategic critical materials [1,2] As REEs, their alloys and compounds possess important technological properties, and therefore, they are applicable in many areas of modern energy technology. Since the demand for some REEs can be estimated, there might be a supply risk. This thesis focuses on the development of a novel recovery method for REEs from Estonian phosphorite ore using liquid extraction followed by electrochemical separation.

Liquid extraction is a chemical separation method when two immiscible liquid phases are brought into the contact immiscible liquid phases are brought into immiscible liquid phases are brought into contact, and some elements transfer from one phase to another. By changing the extraction conditions, extraction results can be tuned in a desirable way.

Electrodeposition is a method of gathering different elements into a working electrode during electrochemical reduction. Electrodeposition results can mainly be tuned by electrolyte composition and applied voltage.

The main aims of this study were:

a) Propose optimal methods for separation of REEs from phosphorite ore using liquid extraction [I, III]

b) Study the mechanism of electrodeposition when a stock solution of one selected element had been used and perform successful electrodeposition of that element [II]

c) Study the mechanism of electrodeposition when preliminary purification of natural phosphorite ore had been performed and perform successful electrodeposition of selected element [III]

The different combined processes were characterized by inductively coupled plasma spectroscopy (ICP-MS), cyclic voltammetry (CV), electrochemical impedance spectroscopy (EIS), chronoamperometry, energy-dispersive X-ray spectroscopy (EDS), atomic emission spectrometry (AES) and scanning electron microscopy (SEM).

4. LITERATURE OVERVIEW

4.1. Rare earth elements

Rare earth elements (REEs) are strategic critical materials [1,2] as they possess important electrocatalytic [3], optoelectronic [4], permanent magnetic [5], and advanced energy storage properties [6,7]. Therefore, REEs are applicable in many areas of modern energy technology, including solid oxide energy conversion devices (fuel cells and electrolysis cells) [8–10], information technology, transport systems (fuel cell components and catalysts for soot combustion), and chemical technology including catalytic reforming of crude oil to gasoline and diesel fuels, metal organic chemistry etc. The application of REEs is increasing even more quickly in industry because all traditional and novel industrial applications are using more and more REEs, examples of which include wind turbines, photovoltaic perovskite type devices, efficient dc motors, explosion-free hydrogen storage complex metal hydrides, fuel cells and electrolyzers (polymer electrolyte membrane and solid oxide fuel cells and electrolyzers, alkaline and direct methanol fuel cells), **c**omplex catalysts for traditional gasoline, diesel production, as well as for modern chemical polymers, synthetic fuel industry and bioelectrochemical devices.

The estimated production of rare earth metal oxides was 350,000 metric tons in 2023. Heavy rare earth elements (HREE) are in much bigger demand compared to light rare earth elements (LREE) (such as lanthanum and cerium). For example, in 2020, there were nearly one billion cars; thus 700,000 tons of Nd is needed only to replace this number of cars one day.

China has been and is the world's greatest supplier of REEs, which may influence supply stability. To overcome any supply risk, we need to develop and implement high-technology recovery alternatives [11–14], as well as more environmentally friendly raw material processing [15–19].

Traditionally, REEs are separated by molten salt electrolysis or liquid extraction methods, which create adverse environmental and economic impacts. Molten salt electrolysis causes significant electricity consumption by generating huge quantities of CO_2 equivalents. Traditional hydrometallurgical methods create water and soil contamination, and a significant amount of organic solvent waste needs to be disposed of. Modern scientific research in this field focuses on finding less harmful alternatives, such as the use of ionic liquids for the treatment of REEs.

In addition to recycling different REE-containing devices, recovery from phosphate rock minerals might relieve an increasing demand for some REEs. REEs have been observed in many phosphate rocks, mainly in monazite, xenotime, loparite, apatite, and ion-absorbed clay [18,20,21]. Some researchers have pointed out that phosphate rock might be a new source for REEs due to its huge, about 300 billion tons reserves worldwide [12,22–24]. The chemical composition of phosphorite is complex since [25–30], along with REEs, significant numbers of

calcium and phosphorus trace elements (d-metals, sp-metals, distributed rare metals) occur at various levels in phosphate rock. Some heavy REEs (HREEs) existing in phosphate rock are highly desired. For the efficient separation of HREEs, light REE, along with Y and most other trace elements, should at first be separated during the phosphorite ore processing stage [31–36].

Estonia has the biggest, though unexploited, phosphorite ore deposits in Europe. These resources might be exploitable commercially for phosphate fertilizer production, but results of the current study indicate that some chemical elements (U, Th, Tl) should be separated from Estonian phosphorite as byproducts before producing the phosphorus fertilizers.

Removing REEs from phosphorite ore is also important from the point of view of environmental and food safety. The dissolution of phosphorite fertilizers is slow, and some toxic and radioactive cations tend to accumulate in the soil [37–40], which is why stricter regulations are being established.

4.2. Ionic liquids

The ionic liquids (IL) are compounds composed solely of cations and anions in liquid state below 100 °C[41,42]. Salts that are liquid at room temperature are called room-temperature ionic liquids (RTIL). ILs are considered environmentally friendly reactants and can be used for the extraction of REEs from solutions of natural ores [43].

Novel ionic liquid-based extraction methods of REEs, combined with unique complex forming agents such as well-designed multi-dental ionic liquids, from pre-treated enriched raw complex mineral acidic solutions, have been under intensive development since 1990 [44,45]. However, the application conditions for novel extraction methods have only been developed for some REEs. In addition, the kinetics of complex formation and extraction have been under-studied in the literature, with relatively few current studies and analyses available. However, kinetic information plays an important role in selecting well-working equipment and separation conditions for the design of industrial production lines[46,47].

It should be stressed that it is possible to perform electrolysis at 60–90 °C, thus at a much lower temperature. This reduces the environmental impact and increases the energy efficiency of REEs production and the final cleaning process. Some selected ILs show good electrochemical stability over a wide potential range. Ionic liquids are also a good alternative because they do not release hydrogen during electrolysis. One more possible advantage of ILs is the versatility and possibility to synthesize ILs with unique properties, thus enhancing the selectivity of the extraction and electrolysis process [43]. The ionic liquids can be cleaned and restored using strong mineral acids and thus applied many times.

At present, electrolysis in ILs is primarily conducted in laboratory-scale research or as part of pilot projects since numerous obstacles must be overcome before any large-scale industrial application in the REEs industry is feasible

[48,49]. Many ILs are moderately expensive. Despite their high electrochemical stability, redox processes occur during electrolysis, which degrade the ILs. Some researchers have recently reported electrodeposition of various rare-earth metals using a bis-trifluoromethylsulfonylimide ($TFSI^-$)-based ionic liquid. Experiments have been conducted within the temperature range from room temperature to 100 °C [50,51]. Different materials have been used for the working electrode, including copper, platinum and glassy carbon [52–55]. Pyrrolidinium- or phosphonium-based ILs have been employed [55,56]. In this research, a pyrrolidinium-cation-based ionic liquid has been chosen due to its high cathodic stability [57,58].

4.3. Processing methods for rare earth elements

4.3.1. Hydrometallurgical route

Extensive literature analysis about REE processing and recovery shows that the first studies in phosphate rock processing were made in the Soviet Union about 90 years ago [21,59]. Since that time, the acid leaching with sulfuric acid, nitric acid, hydrochloric acid and phosphoric acid has been developed, followed by different recovery routes such as crystallization and precipitation, ion exchange and multistep solvent extraction. The issue with sulfuric acid is that it forms phosphogypsum, trapping 50–65% of REEs, and only 50–35% of REEs will be collected into the phosphoric acid aqueous solution Extraction of REEs from phosphogypsum is a very complicated multistep process (treatment with concentrated KOH for initial dissolution of phosphogypsum, thereafter with concentrated HNO_3.) being a time and energy consumption process generating moderate quantities of waste.

The solvent extraction method seems to be the most promising technology for large-scale environmentally friendly REEs separation since other methods consume a lot of energy, generate huge quantities of waste products, and the collected REEs contain different impurities [60,61].

It should be noted that the separation of an individual REE is a very complicated, energy- and time-consuming task [62,63]. During the liquid extraction process, many other elements co-extract together with REE; the most noticeable example is the co-extraction of uranium and thorium [64]. These elements threaten the environment and nutritional safety if they are not removed during phosphate rock processing for phosphorite fertilizers. Some researchers have reported co-extraction of radioactive elements together with REE [65,66]. Some research groups have conducted extraction experiments with natural phosphate rock acid leachate, while some research groups use REE stock solutions, which represent the content of REEs in natural phosphate rock [15,18,21,25,67]. As the current study indicates, extraction results, thus extraction efficiency and separation factors, obtained and calculated for stock solutions are not always comparable with extraction

results from phosphate rock acid leachate due to the different complicated chemical composition of solution prepared by dissolution of phosphate rock in HNO_3, HCl or HNO_3+ HCl aqueous solutions. The chemical content of natural phosphate rock is significantly more complicated, and systematic studies are inevitable for the separation and extraction of all useful elements.

Estonian phosphorite ore contains at least 59 trace metal elements along with residual mineral materials [29]. In order to achieve preliminary separation of REE from other elements, liquid extraction was performed. Liquid extraction is a rapid and cost-effective method for initial separation of different elements before applying electrochemical techniques [68].

Liquid extractant such as bis(2-ethylhexyl) phosphate (D2EHPA) can be used for separating REE from phosphorous ore acid leachate [69]. Nitric acid, hydrochloric acid leachate was used during current experiments. Depending on acidity of leachate, different REEs can be separated from each other. In more acidic leachate, higher atomic mass HREE transfers to an organic phase, leaving light REE elements into a water phase. Therefore, liquid extraction began with a more acidic solution to transfer higher REE to the organic phase and isolate them from light REEs. The water phase with lighter REEs was dry evaporated. The dry material was dissolved again in less concentrated HNO_3 acid and extracted with D2EHPA. Stripping from D2EHPA to the water phase can be performed with concentrated nitric or hydrochloric acid. REEs (tri)nitrates or tri(chlorides) can be obtained after dry evaporation of the water phase. For electrochemical cleaning process, obtainment of trinitrates was preferred.

Many other elements can be eliminated from raw material during liquid-liquid extraction. Especially important is the removal of radioactive uranium and thorium [70–72], to increase the safety of handling the REE materials. However, 1iquid extraction is not entirely selective. Many other elements remain with REEs. For example, calcium is a major element in phosphorite ore, and it remains a major element in trinitrate salts after extraction and stripping. In order to remove different elements from REE, electrochemical separation was conducted [73].

4.3.2. Electrochemical route

Traditionally, clean rare-earth metals are produced industrially using molten salt electrolysis [74–76]. This process is highly energy-intensive since very high temperatures are required [77]. An alternative route is to perform electrolysis from room-temperature ionic liquids (ILs) [78,79]. ILs are considered to be environmentally friendly [45,80,81] and it is possible to perform electrolysis at lower temperatures (up to 100 °C), reducing the environmental impact. ILs also show good electrochemical stability over a wide potential range [45,82,83]. For final cleaning and deep separation of individual REEs, usually high-temperature electrolysis in eutectic mixture of LiCl + KCl (at 680–900 °C) has been used, needing once again huge quantities of electricity. REEs cannot be electrolyzed from the water solution due to hydrogen evolution occurring at less negative potential compared to the reduction potential of REE cations.

Electrodeposition of REEs requests the use of a non-aqueous electrolytic medium, such as molten salts, organic solvents, or ionic liquids (ILs) [53,84–87]. Molten salt electrolysis of REEs is a branch of pyrometallurgy and is currently the primary process for REEs production [88]. Molten salts were studied due to their potential benefits, including high solubility, diffusion coefficient, conductivity, low viscosity, and rapid electrode reaction. However, they have high corrosion activity and high energy consumption due to high-temperature operation. Therefore, organic solvent-based electrolytes are also sometimes selected as electrolytes for electrodeposition of REEs. The characteristics of organic solvents are as follows: they have large polarizability, good conductivity of solutions, high concentration of metal ions in solution, moderate to high current efficiency, and low cost. Furthermore, organic solvent solutions, in comparison with aqueous solutions, offer several unique advantages. These include no impact on hydrogen production, high activation energy for reaction with an active electrode material, and sometimes easy electrodeposition of REE metals. Nevertheless, they are generally poisonous, inflammable, and volatile and have a low conductivity, limiting their applications [77].

Regarding electrodes, most previous studies have used either copper or platinum working electrodes. In this study, a polycrystalline gold electrode and platinum electrode were utilized as the working electrode to enhance surface catalytic effects [89].

4.4. Electrochemical characterization techniques

4.4.1. Cyclic voltammetry

Cyclic voltammetry is commonly used as the first electrochemistry experiment to acquire qualitative and quantitative information about electrochemical systems [90,91]. In the CV method, the electrode potential, E, is cycled with a constant scan rate between most negative and most positive designated potential values, and the current value is recorded. The resulting current vs. potential plot, the cyclic voltammogram, gives an overview of the reduction or oxidation processes of electrochemically active species at the interphase of working electrode and electrolyte [92].

4.4.2. Constant potential technique

An instrument known as a potentiostat has control of the voltage across the working electrode-counter electrode pair, and it adjusts this voltage to maintain the potential difference between the working and reference electrodes (which it senses through a high-impedance feedback loop) in accord with the program defined by a function generator. One can view the potentiostat alternatively as an active element whose job is to force through the working electrode whatever current is required to achieve the desired potential at any time. Since the current and

the potential are related functionally, that current is unique. Chemically, it is the flow of electrons needed to support the active electrochemical processes at rates consistent with the potential. Thus, the response from the potentiostat (the current) actually is experimentally observable.

In general, a controlled fixed potential experiment carried out for the electrode reaction

$$O + e \underset{k_b}{\overset{k_f}{\rightleftarrows}} R \tag{1}$$

where O stands for oxidized form and R for reduced form of the standard system, k_f heterogeneous rate constant for reduction and k_b heterogeneous rate constant for oxidation, can be treated by invoking the current-potential characteristic:

$$i = Fak^0[C_O(0,t)e^{-\alpha f(E-E^{0'})} - C_R(0,t)e^{(1-\alpha)f(E-E^{0'})}] \tag{2}$$

where F stands for Faraday constant, A area of the electrode, k_0 standard heterogeneous rate constant, C_O concentration of oxidized form and C_R concentration of reduced form and α transfer coefficient.

In conjunction with Fick's laws, which can give the time-dependent surface concentrations $C_O(0, t)$ and $C_R(0, f)$. Therefore the faradic processes characteristics can be established and analyzed. [92,93]

4.4.3. Electrochemical impedance spectroscopy

Electrochemical impedance spectroscopy and alternating current impedance method have grown in popularity in recent years [94–98]. Initially applied for the determination of the EDL capacitance and in AC polarography, nowadays they are often applied to characterize processes at complex interfaces. Electrochemical impedance spectroscopy (EIS) studies the system response to the application of a periodic small amplitude AC voltage signal by measuring the current through the electrochemical cell. Analysis of the system response contains information about the interface, its structure and reactions taking place at the interface [99,100].

During the experiment sinusoidal perturbations are applied to the electrochemical system:

$$E(t) = E_0 A \sin(\omega t), \tag{3}$$

where E(t) is the potential at time t, EA is the potential amplitude, ω is the angular frequency with a relationship to frequency f in Hz: $\omega = 2\pi f$. The current response I(t) will be a sinusoid at the same frequency but shifted in phase in case of capacitive or inductive interfaces:

$$I(t) = I_0 A \sin(\omega t + \varphi), \quad (4)$$

where I(t) is the current at time t, IA is the current amplitude and is phase angle shift by which the voltage follows the current. According to the Ohm's law, the impedance is defined as the ratio of voltage and current

$$Z = E(t)/I(t). \quad (5)$$

Impedance has magnitude and phase angle and thus is a vector quantity. Therefore, it is convenient to be presented as

$$Z = Z_0 A (\cos \varphi + i \sin \varphi) = Z' + iZ'', \quad (6)$$

where $i = \sqrt{-1}$, Z' is real part of impedance, and Z'' the imaginary part of the impedance [100–102].

The EIS method is destructive in principle, meaning that a small AC voltage signal is applied to the interface which induces a counteracting AC current to stabilize the interface. By applying signals of differing frequencies, processes taking place with different time constants can be probed. In general, for electrochemical systems, three main non-distributed fundamental processes that can be ascribed are: resistive (such as faradic charge transfer) corresponding to a 0-degree phase shift between the voltage and current signals; diffusion (such as classical Fick'ian semi-finite length diffusion of reactants) corresponding to a –45-degree phase shift, and capacitive (such as purely electrostatic, adsorption rate limited electrical double layer formation with capacitance C) processes that show a –90-degree shift between the AC voltage and current signals. The dependence of the interfacial resistance on applied signal frequency can be calculated from the measurement and plotted in a complex plane whereby the real part of the resistance $Z'(\omega)$ shows the resistive and the imaginary part $Z''(\omega)$ shows the capacitive part of the interfacial resistance. Calculated complex resistance plots based on certain electrical equivalent circuit (EC) elements can be fitted to the experimental data, with each component representing one physical process that takes place at the electrochemical interface. Dependent upon the measurement quality, each set of data can be described by ECs and the quality of the fit can then be evaluated based on statistical fitting error. Each possible physical process ascribed to an interface can be represented as a separate element (or combination of elements for diffusion) in the overall equivalent scheme and its validity can be tested based on its effect on the overall fitting error. If the addition of a free variable does not decrease the overall fitting error by at least 50%, it is considered to not be a descriptive part of the overall equivalent scheme that characterizes the interfacial processes [103]. By ascribing all the possible physical processes that can occur at the interface and testing their validity, one can derive an overall equivalent scheme that best fits the measurement results and thus the occurring interfacial processes.

4.5. Microscopic and spectroscopic characterization techniques

4.5.1. Inductively coupled plasma mass spectroscopy (ICP-MS) and microwave plasma atomic emission spectroscopy (ICP-AES)

Inductively coupled plasma spectroscopy (ICP-MS) and microwave plasma atomic emission spectroscopy (ICP-MS) are powerful methods for the detailed chemical analysis of samples with complex chemical compositions and structures. ICP-MS and ICP-AES can be used for the quantitative analysis of different metal cations in acidic solutions of phosphorite ore, as well as in extracted solutions of various REEs in stripped aqueous solution. For the detailed quantitative analyses, the standard solutions will be measured to calibrate the device. The samples have been prepared using 2% aqueous HNO_3 and the metals concentration around 5mg/L have been analyzed using Agilent 4210MP-AES. [30,93]

Major oxides in phosphorite ore can be analyzed via inductively coupled plasma atomic emission spectrometry (ICP-AES) using a Perkin Elmer OPTIMA 3300 RL. The acid digestion can be performed using a mixture of HNO_3-Br_2-HF-HCl. The loss on ignition value was determined when the samples were heated at 1100 °C for 1 h. For potentially toxic metals determination, ~0.25 g of powdered and dried samples were studied via inductively coupled plasma atomic mass spectrometry (ICP-MS) using a PerkinElmer Elan 6100 DRC after digestion in a mixed solution ($HClO_4$-HNO_3-HCl-HF). The analytical values obtained were within the 95% confidence limits of the recommended values for this certified material.

4.5.2. XRD and XRF methods

X-ray diffraction is the simplest and quickest method for characterizing the surface structure, structural phases and crystallographic structure of the deposited rare earth metal layer and the working electrode before the electrodeposition of REEs [104]. XRD can be used to identify metal phases, oxides, carbides, or metal nano-structural deposits on carbon, gold, and stainless steel electrodes.

The effective crystallite size d(Scherrer) can be estimated from the diffraction pattern of the powder. Rare earth metal layers deposited can be visualized by scanning electron microscopy (SEM) and analysed for chemical composition using X-ray energy dispersive (EDX) methods. Metal layers and particles deposited can be more accurately visualized at a nanometer scale using high-resolution transmission electron microscopy (TEM) in combination with selected area electron diffraction (SAED) or electron energy loss spectroscopy methods (EELS). Another powerful method for investigating the deposited material is Raman spectroscopy, which can be used for the detailed characterization of different carbon working electrodes before the electrodeposition of REE or REE – Bismuth alloys. For chemical analyses, X-ray fluorescence spectroscopy (XRF) can be used [105].

5. EXPERIMENTAL

The overall conception of the experimental part is depicted in Fig 1. Phosphorite ore is leached in strong nitric or hydrochloric acid and then filtered. Preliminary leachate purification involves liquid-liquid extraction to separate REEs from other elements. Different groups of REEs can be separated depending on extraction conditions. After the stripping step, the rare earth elements transfer to aqueous phase and can be collected by water evaporation. Some other elements remain in the dry material and need to be further separated. This study proposes electrochemical purification. The dry material obtained is dissolved in an electrolyte solution containing ionic liquid and Bi^{3+} ions. Rare earth elements are separated from other elements by electrodeposition. A bismuth and REE bi-metallic layer form on the working electrode surface. The final separation of Bi from REEs needs to be done.

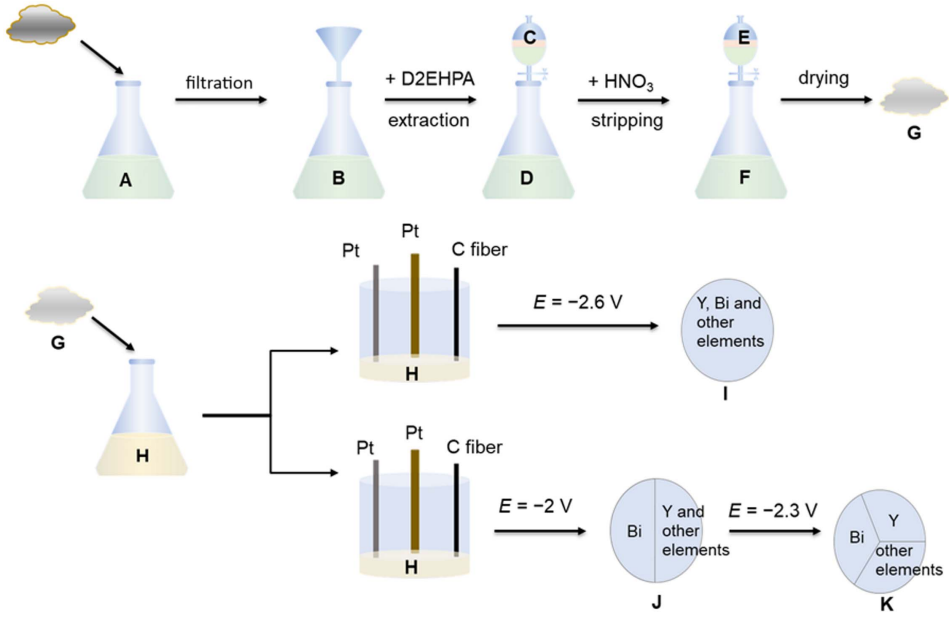

Figure 1. Overall separation process of REE from phosphorite ore natural sample starting from liquid extraction of raw material to the electrochemical separation.

5.1. Liquid extraction

5.1.1. Raw materials and chemicals in liquid extraction experiments

Samples of concentrated phosphorite ore from Estonian Iru outcrop were obtained from geological collections of Tallinn University of Technology, and samples of Ülgase outcrop were obtained from geological collections at the Institute of Ecology and Earth Sciences, University of Tartu. Trioctylmethyl ammonium chloride (Aliquat 336), HNO_3, bis(2-ethylhexyl) phosphate (D2EHPA) and NaOH were purchased from Merck. HCl was purchased from Honeywell and KNO_3 was purchased from Lach-ner. (All chemicals had the purity of analytical grade.) The structure of the extractants is depicted in Figure 2.

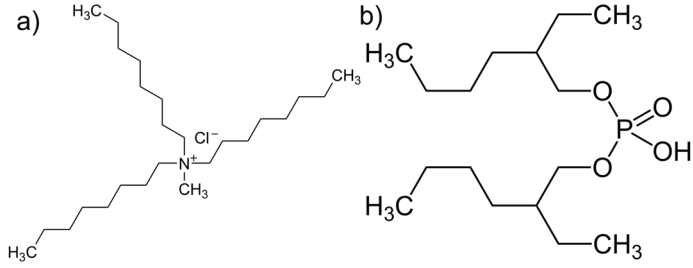

Figure 2. The structures of (a) trioctylmethyl ammonium chloride (A336) and (b) bis(2-ethylhexyl) phosphate (D2EHPA).

5.1.2. Modification of Aliquat 336 with 2.5 M KNO_3

To achieve better selectivity for REEs and reduce extractant viscosity for quicker mass transfer, Aliquat 336 was treated with potassium nitrate to exchange Cl^- with NO_3^-. In most cases, A336[NO_3] was diluted with an organic solvent such as n-heptane, xylene, or kerosene [15,106]. However, undiluted A336[NO_3] has also been used, as in the paper by Larsson and Bienemans [18]. In addition to extracting REEs, A336[NO_3] has also been used to extract other metals like vanadium from chromium-containing solutions [107]. To prepare A336[NO_3], Aliquat 336 was pre-equilibrated 3 times with 2.5M KNO_3 for at least 1 h each time.

5.1.3. Feed solutions in liquid extraction experiments

In our experiments, we used two various phosphorite ore solutions and one REE[NO_3]$_3$ stock solution to test our extraction technology:

a) In the first experiment, a phosphorite ore solution and a REE[NO_3]$_3$ stock solution were made. For phosphorite ore solution, 2.46 g of concentrated phosphorite powder from Estonian Iru deposit was dissolved in 100 mL 7.5M HNO_3 aqueous

solution for 24h at room temperature. The solution was then filtered to remove any undissolved substances. For $REE[NO_3]_3$ stock solution, $REE[NO_3]_3$ trinitrate salts were dissolved in dilute nitric acid to prepare a 1-liter solution with a pH of 1.5. The pH of the stock solution was measured using an Elmetron pH meter CP-411. The compostitions of the stock solutions prepared from selected $REE[NO_3]_3$ salts are listed in Table 1.

Table 1. List of millimolar concentrations of selected REEs in $REE[NO_3]_3$ salt stock solution used for testing extraction performance of $A336[NO_3]$.

REE trinitrate salt	Concentration
$La(NO_3)_3 \bullet 6H_2O$	0.94 mM
$Ce(NO_3)_3 \bullet 6H_2O$	0.98 mM
$Pr(NO_3)_3 \bullet 6H_2O$	0.69 mM
$Gd(NO_3)_2 \bullet 6H_2O$	0.60 mM
$Tb(NO_3)_3 \bullet 6H_2O$	0.69 mM

b) In the second experiment, a 10.5 g sample of phosphorite ore powder from the Ülgase deposit was dissolved in 100 mL of 3 M hydrochloric acid.

5.1.4. Equipment

For the quantitative analysis, REEs and trace elements in untreated solution and extracted solution samples have been established using Agilent 8800 QQQ ICP-MS in NoGas mode regime. Various metal cations such as 45Sc, 89Y, 137Ba, 139La, 140Ce, 141Pr, 146Nd, 147Sm, 153Eu, 157Gd, 159Tb, 163Dy, 165Ho, 166Er, 169Tm, 172Yb, 175Lu, 232Th and 238U have been quantified from aliquots diluted 400-fold with 2% HNO_3 aqueous solution before analysis. All extraction experiments were carried out in 100 ml plastic separation funnels.

5.1.5. Experimental conditions

a) Experimental conditions during the first liquid extraction experiment.

The main focus of this study has been on the extraction efficiencies of undiluted nitrated Aliquat 336 ($A336[NO_3]$) and undiluted D2EHPA has been the focus of this study. In the first extraction step, samples of concentrated Estonian phosphorite ore were dissolved in 7.5M nitric acid and then extracted using undiluted $A336[NO_3]$ or undiluted D2EHPA. The aqueous feed solution and extractant were consistently maintained at a 9:1 (aqueous/organic) ratio in all cases. The mixture was shaken carefully in a separation funnel for 1 min and then kept silent for 1 h to reach equilibration. The resulting raffinate was extracted 2 more times with a fresh amount of $A336[NO_3]$ to facilitate a more thorough extraction of U, Th, and Tl.

Reaction equilibrium for A336[NO_3] extraction can be expressed as Eq. 7:

$$M^{3+}(aq) + y(R_3N^+CH_3)NO_3^-(IL) + 3\ NO_3^-(aq) \rightleftarrows (R_3NCH_3)M(NO_3)_{y+3}\ IL \quad (7)$$

Where M^{3+} designates the metal cation, $(R_3N^+CH_3)NO_3^-{}_{IL}$ represents A336[NO_3] and $(R_3NCH_3)M(NO_3)_{IL}$ represents metal cation and ionic liquid complex. IL represents ionic liquid phase and aq aqueous phase.

Equilibrium constant K can be rewritten as:

$$K_{eq} = \frac{(R_3NCH_3)M(NO_3)_{y+3\ IL}}{M^{3+}(aq)\ [(R_3N^+CH_3)NO_3^-(IL)]^y + (NO_3^-)^3\ (aq)} \quad (8)$$

Reaction equilibrium for D2EHPA extraction can be expressed as Eq. 9:

$$M^{3+} + 3\ [HA]_2 \rightleftarrows [MA_3(HA)_3] + 3\ H^+ \quad (9)$$

Where M^{3+} represents the metal cation, [HA] is the extractant in the organic phase; and $[MA_3(HA)_3]$ represents the metal-extractant complex in the organic phase.

Equilibrium constant K_{eq} can be rewritten as:

$$K_{eq} = \frac{[MA_3(HA)_3]+[H^+]^3}{M^{3+} + [(HA)_2]^3} \quad (10)$$

Only one extraction step was performed with D2EHPA due to the very high extraction efficiency achieved. In the next step, raffinate was saponified with 1M NaOH to reach a pH of 1.5, and then REEs were extracted once again using the same extractant. The raffinate sample was quantitatively characterized after each extraction step using the ICP-MS (Inductively Coupled Plasma Mass Spectrometry) measurement method. A comparative parallel extraction experiment was conducted using a stock solution (i.e., a mixture of different REE[NO_3] salts with a precisely known chemical composition) in order to quantitatively control the results obtained for REE tests. REE[NO_3] salts were dissolved in moderately diluted nitric acid (pH of a solution was 1.5) and extracted with A336[NO_3]. No further experiments with obtained materials were performed after the first liquid extraction experiment.

b) Experimental conditions during the second liquid extraction experiment.

The study has focused on the separation of Y and REEs from natural phosphorite ore samples, followed by Y separation from other REEs.. The 10.5g sample of phosphorite ore from the Ülgase deposit was dissolved in 3 M hydrochloric acid aqueous solution for 5 min at room temperature and then filtered to remove any undissolved substances to prepare an acidic feed solution. A total of 50 mL of acidic feed solution was extracted with 5 mL of D2EHPA using a plastic separation funnel. The mixture was shaken for 1 min and then left undisturbed for 15 min to equilibrate. The D2EHPA solution of REEs and Y, obtained from the

extraction stage, was transferred to a new separation funnel and stripped with 50 mL of concentrated nitric acid. The solution mixture was shaken for 1 min and then left undisturbed for 15 min to equilibrate.. The aqueous phase was separated, H_2O was evaporated, and nitrates of various elements were obtained. Aqueous phase samples were collected before and after the extraction as well as after the stripping experiment, to conduct the ICP-MS measurements. A mixture of different nitrates obtained from stripping was used in the electrochemical experiments.

Reaction equilibrium and equilibrium constant for D2EHPA extraction can be expressed as Eqs. 9 and 10, respectively.

5.2. Electrochemical separation

Electrochemical separation has been conducted in two different sets of experiments. In the first set of experiments our proposed electrodeposition method was tested. Pr trinitrate salt was dissolved in a mixture of propylene carbonate and ionic liquid, and after the electrochemical studies, Pr was reduced to the working electrode in the metallic state. In the second set of experiments, a dry material obtained after the liquid extraction of the phosphorite ore and stripping was electrochemically studied. For practical reasons, Y separation was conducted from other REEs. All experiments must yield an answer regarding the possibility of electrochemically separating individual REE elements or element subgroups after conducting preliminary purification of phosphorite ore during the liquid extraction phase.

Another crucial question pertains to the significance and role of Bi cations in the electrolyte solution, enabling the reduction of any REE at the working electrode surface.

5.2.1. First set of experiments – electrochemical separation of praseodymium from praseodymium trinitrate salt

5.2.1.1. Three-electrode electrochemical cell

A mechanically polished polycrystalline gold disk with a surface area of 0.2 cm^2 was used as the working electrode, a high surface area Pt net served as the counter electrode, and carbon fiber served as the pseudo-reference electrode. All measurements were carried out in a three-electrode electrochemical cell at a constant temperature of 298 K (room temperature) unless otherwise stated.

5.2.1.2. Electrolyte

For detailed calibration, praseodymium trinitrate hexahydrate (99.9% trace metal basis, Sigma-Aldrich) was dried under an argon atmosphere at 100 °C for 24 h to remove as much residual water as possible. Bismuth(III) trifluoromethanesulfonate ($Bi(OTf)_3$, 99%) was purchased from Alfa Aesar. 1-Butyl-1-methylpyrrolidinium bis(fluorosulfonyl)imide (BMPyrrFSI), (99.5%, $H_2O < 50$ ppm, Solvionic) was used as a solvent and electrolyte for the electrochemistry experiments.

5.2.1.3. Electrochemical characterization

Cyclic voltammetry and electrochemical impedance spectroscopy were used to investigate the electrochemical characteristics of the system using an Autolab PGSTAT 320 with FRA II. All measurements were carried out inside a glove box MBRAUN LabMaster 130 Glovebox (H_2O < 1 ppm, O_2 < 1 ppm). Electrochemical impedance spectroscopy measurements were performed first, then the cyclic voltammetry experiments, and finally the electroreduction of Bi and Pr cations in chronoamperometric mode. Potential cycling rates up to 50 mV/s were applied. Impedance spectra were measured within the frequency range from 10^{-1} to 10^4 Hz with a 15 mV ac modulation amplitude.

5.2.2. Second set of experiments – electrochemical separation of yttrium from other REEs using phosphorite ore as the starting material

5.2.2.1. Raw materials and chemicals

Samples of Estonian concentrated phosphorite ore from Ülgase outcrop were acquired from geological collections of the Institute of Ecology and Earth Sciences at the University of Tartu.

HNO_3 was purchased from Sigma-Aldrich, HCl from Honeywell, bis(2-ethylhexyl) phosphate (D2EHPA) from Merck, propylene carbonate (PC) from Sigma-Aldrich, bismuth(III)trifluoromethanesulfonate ($(Bi(OTf)_3$, 99%) from Alfa Aesar and (BMPyrFSI) from Solvionic, (99.95%, H_2O <50 ppm). All chemicals have the purity of analytical grade, unless otherwise specified. Structures of PC, $Bi(OTf)_3$ and BMPyrFSI have been presented in Figure 3.

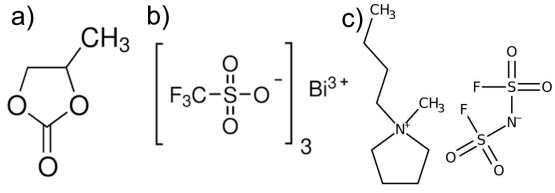

Figure 3. Structures of chemical compounds used in electrochemical separation. a) Propylene carbonate b) Bismuth trifluromethanesulfonate ($Bi(OTf)_3$) c) 1-Butyl-1-methylpyrrolidinium Bis(fluorosulfonyl)imide.

5.2.2.2. Feed solution

0.12 g dry evaporated sample obtained from the liquid extraction using D2EHPA was dissolved in 3 ml propylene carbonate. 0.09 g (50 mM) $Bi(OTf)_3$ was added and dissolved, finally 0.18 g (0.2 M) BMPyrFSI was added to the solution and dissolved. The solution was prepared under the argon atmosphere in the glovebox at room temperature. The solution was then used in electrochemical deposition experiments. For the higher selectivity of electrochemical deposition

experiments, the dry evaporated sample mass was lowered to 0.03 g while the Bi concentration was lowered to 10 mM.

5.2.2.3. Equipment

For the quantitative analysis of REEs and trace elements in untreated solution and extracted solution sample have been established using Agilent 8800 QQQ ICP-MS in N_2O gas mode regime.

Electrochemical measurements were carried out in a three-electrode electrochemical cell at room temperature. Chemically purified Pt, modified in situ with a Bi electrodeposited layer from $Bi(OTf)_3$ solution, was used as the working electrode. A high surface area Pt net served as the counter electrode, and carbon fiber was used as the pseudoreference electrode.

The cyclic voltammetry and electrochemical impedance spectroscopy methods were used to investigate the electrochemical characteristics of the completed electrochemical system using Autolab PGSTAT 320 with FRA II. All measurements were carried out inside a glove box MBRAUN LabMaster 130 Glovebox (H_2O < 1 ppm, O_2 < 1 ppm) filled with Ar.

5.2.2.4. Experimental conditions

Dry material was transferred to the glove box under the argon atmosphere and heated additionally inside the glovebox at 70 °C for 24 hours to remove residual water as much as possible. Then the material was cooled down to room temperature before being dissolved in propylene carbonate inside the glass vial. The mixture was stirred with a magnetic stirring bar at 600 rpm for 1 hour to dissolv the solid material (REEs). ($Bi(OTf)_3$ was then added and stirred for 1 hour. Finally, ionic liquid (BMPyrFSI) was added and stirred for 15 minutes.

After dissolution, the mixture was transferred into an electrochemical cell for electrochemical experiments. Electrochemical impedance spectroscopy measurements were performed at first, the CV curves were then recorded, and finally, the electroreduction of Bi and Y cations in chronoamperometric mode was performed. Potential cycling CV curves were measured at potential scanning rate of 50 mV/s, and impedance spectra were measured within alternative current frequency range from 0.01 to 10 000 Hz with 15 mV ac modulation amplitude. Cathodic potentials of –2.0, –2.3 and –2.6 V were applied during electroreduction at chronoamperometric mode for 24 h. Samples of solution were taken before and after electrochemical experiments for detailed ICP-MS analysis.

5.3. Microscopic and spectroscopic analysis

Electron microscopy was performed in high vacuum mode using a Zeiss Evo MA15 variable pressure electron microscope equipped with an Oxford AZTEC energy dispersive X-ray spectroscopy (EDS) detector. Microwave plasma atomic emission spectroscopy (MP-AES) was performed using an Agilent 4210 MP-AES.

6. RESULTS AND DISCUSSION

6.1. Liquid extraction

6.1.1. First extraction step for U, Th, and Tl removal from concentrated nitric acid media

6.1.1.1. Extraction with A336[NO_3]

Results of the current study indicate that it was possible to extract U, Th, and Tl from the concentrated nitric acid medium using A336[NO_3]. The cumulative extraction efficiencies after three consecutive extractions were 85% for uranium, 66% for thorium, and 99% for thallium [29]. The extraction process was very selective for U, Th and Tl, with no co-extraction of other elements. However, the extraction efficiencies of REE were significantly smaller compared to those established using D2EHPA. The only exception was thallium, which was extracted only by nitrated Aliquat 336. From this, it can be concluded that Aliquat 336[NO_3] is suitable, but not the best option for removing U, Th, and Tl. The extraction of REEs from concentrated nitric acid media using A336[NO_3] has been discussed by Kumari et al. [17]. It has been suggested that the use of EDTA (ethylenediaminetetraacetic acid) promotes the extraction of REEs. Since no complexing agents were used in the current study, low REE extraction efficiency can be a result.

6.1.1.2. Extraction with D2EHPA

The extraction of U and Th was highly efficient in concentrated nitric acid using D2EHPA as an extractant. The extraction efficiency of D2EHPA showed superior extraction efficiency compared to nitrated A336, except for Tl, which was not extracted with D2EHPA at all. Other toxic elements such as Cd, and Pb were not extracted with D2EHPA. However, the extraction selectivity of D2EHPA was not as good as selectivity with A336[NO_3]. Some HREEs were extracted along with U and Th, showing similar extraction behavior. Most REEs were not extracted at all and the selectivity of D2EHPA could still be regarded as very good.

6.1.2. Extraction of REEs from Partially Neutralized Nitric Acid Media

6.1.2.1. Extraction with A336[NO_3]

As these results in Figure 4 show, the extraction efficiency of REEs from partly neutralized nitric acid solution with A336[NO_3] was very low, indicating the A336[NO_3] was not a suitable option for REE extraction. To further investigate the extraction performance of A336[NO_3], some REEs from the stock solution of selected REE nitrate salts were extracted using A336[NO_3]. This time, extraction efficiencies were much higher, with all efficiency values ranging between 57–61%.

The significant differences observed between the real and stock solutions could be explained by the very complicated chemical composition of Estonian phosphate ore, which contains, in addition to U, Th, Tl, and REEs, many other metals. Competitive effects in extraction may occur as a result.

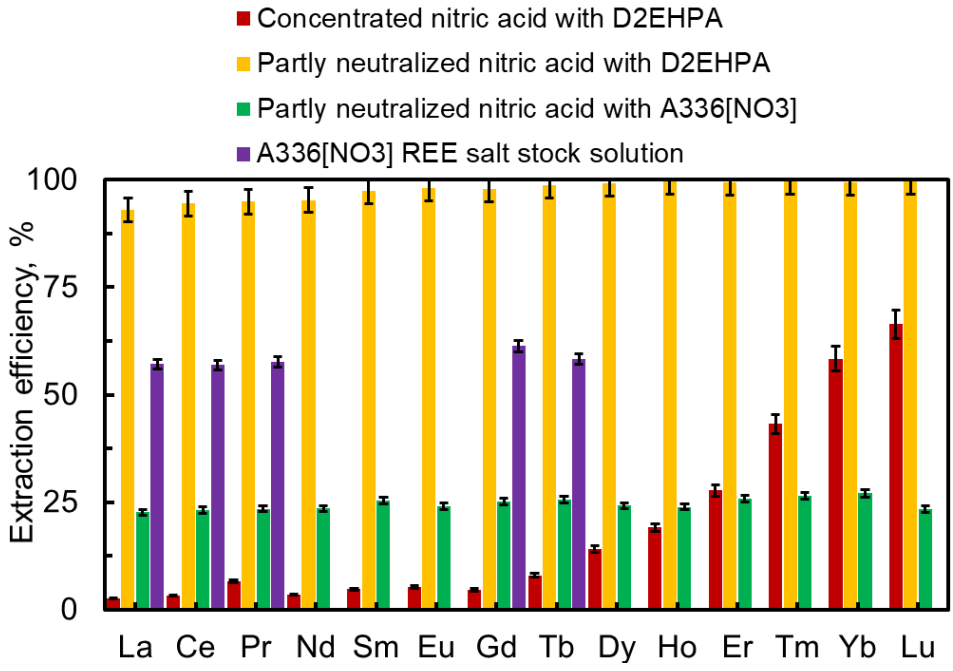

Figure 4. Extraction efficiencies of REEs using D2EHPA and A336[NO_3] as the extractants from phosphorite ore nitric acid solution and extraction efficiency of A336[NO_3] from a stock solution of selected REE nitrates (content described in Table 1. 7.5M nitric acid designates the concentrated acid and raffinate at pH 1.5 value designates diluted nitric acid media. The time of extraction was 1 h. Extraction was performed at room temperature. Undiluted D2EHPA and A336[NO_3] were used as extractants.

6.1.2.2. Extraction with D2EHPA

As these results in Figure 4 show, very high extraction efficiency was calculated for all REEs from dilute nitric acid solution. Extraction efficiency from concentrated nitric acid solution is better for HREE and negligible for LREE. Thus, for selective extraction of HREE, concentrated nitric acid is the best option. It is important to mention that many other elements will be extracted with REE both in dilute and nitric acid media. For the result see Figure 5. Additional separation need to be conducted for selective REE isolation.

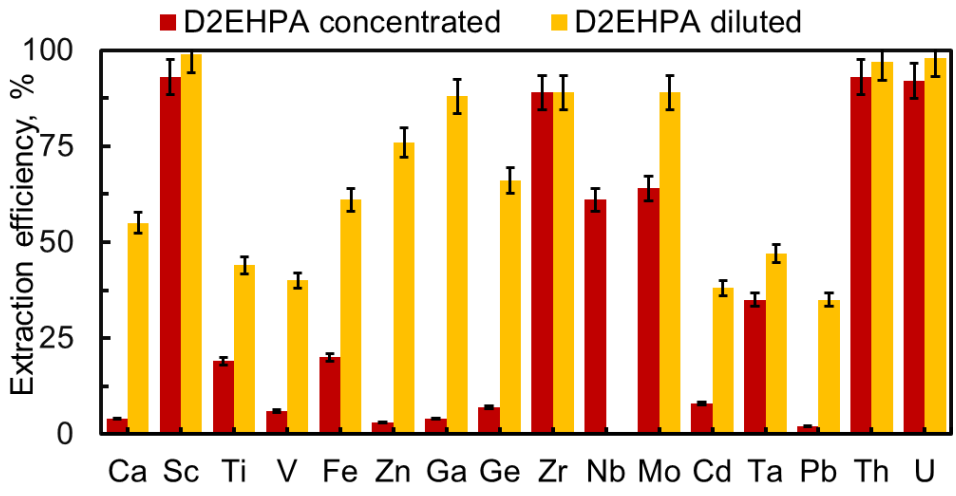

Figure 5. Extraction efficiencies of REE and other selected elements from phosphorite ore concentrated and dilute nitric acid solution using D2EHPA as an extractant. 7.5M nitric acid designates the concentrated acid and raffinate at pH of 1.5 value designates diluted nitric acid media. The time of extraction was 1 h. Extraction was performed at room temperature. Undiluted D2EHPA was used as an extractant.

6.1.3. Extraction of REEs from 3M hydrochloric acid media

As the results in Figure 6 indicate, extraction from 3M hydrochloric acid solution using D2EHPA as extractant separates Y from light rare earth elements (La-Gd) efficiently. Light REEs remain int the aquoeus phase while Y accumulates in the organic phase. Y is one of the major elements in the initial solution, comparable with Ce, Nd and La. All light REEs have remained in the aquoeus phase during extraction, and Y has become a dominant element in the organic phase. Thus, very good separation of Y from other REEs has been achieved during the extraction.

Table 2. Concentrations of Y and other REEs in initial 3M hydrochloric acid aqueous solution and after the extraction in the D2EHPA phase.

Element	C_w initial, ppb	C_{org}, ppb	Element	C_w initial, ppb	C_{org}, ppb
Sc	353	267	**Gd**	5 847	–
Y	36 471	22 371	**Tb**	852	136
La	16 751	-	**Dy**	5 132	1 647
Ce	39 128	-	**Ho**	1 008	487
Pr	4 916	-	**Er**	2 612	1 751
Nd	21 518	229	**Tm**	296	262
Sm	4 479	-	**Yb**	1 441	1 410
Eu	1 037	36	**Lu**	177	176

The concentration of hydrochloric acid has a significant impact on the extraction profile. As it it seen in Figure 6, extraction from less concentrated hydrochloric acid than 3M would increase Y extraction efficiency, while introducing lighter REE into the organic phase. Extraction from more concentrated hydrochloric acid than 3M would introduce more heavy REE to the organic phase, which is an adverse effect for the best Y separation. Thus, for the best Y separation selectivity with acceptable efficiency 3M hydrochloric acid concentration seems to be a good compromise.

Stripping of Y using concentrated nitric acid is not very effective with only 8.5% of Y transferring from the organic phase back to the aqueous phase. The process is also not selective for REEs, as many REE are transferred back to the aqueous phase to some extent. Still, it is worth to noting that most heavy REEs (such as Yb, Lu) mostly remain in the organic phase even when stripping is performed with concentrated nitric acid. Stripping with 7.5M hydrochloric acid would give much higher Y stripping efficiency[29]. Since obtainment of $Y(NO_3)_3$ was preferred for following electrochemical treatment (deposition onto electrodes), nitric acid stripping was performed to improve results through repeated steps.

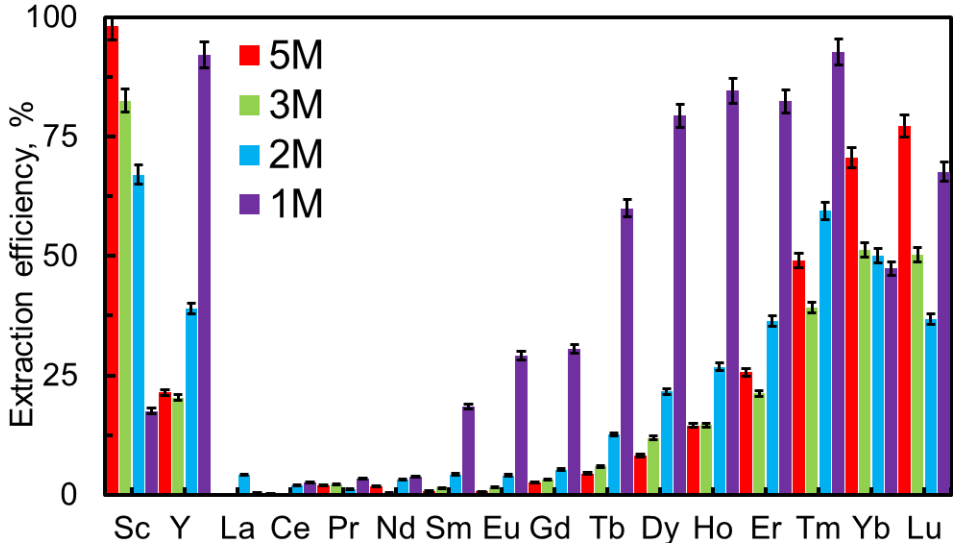

Figure 6. Extraction efficiencies for REEs using D2EHPA as the extractants from phosphorite ore xM hydrochloric acid solution, x denoted in the figure. The time of extraction was 1 h. Extraction was performed at room temperature. Undiluted D2EHPA was used as extractant.

6.1.4. Extraction of other elements than REE from 3M hydrochloric acid media

The phosphorite ore sample contains many elements, so not only Y and REE will be extracted or stripped. Calcium is the major element in natural phosphorite ore samples, and it remains the major element in the dry material obtained after extraction, stripping and dry evaporation. Apart from calcium, elements such as Mg, Al, Fe or Mn are still much more abundant in the natural sample compared to Y. Despite the significant enrichment of Y other elements besides REEs still need to be isolated from Y. Precipitation of Ca is usually not a suitable option since REEs tend to precipitate along with Ca, resulting in no separation. Therefore, for final purification, the electrochemical separation of Y from other elements has been suggested.

6.2. Electrochemical separation

6.2.1. Electrochemical separation of praseodymium from praseodymium trinitrate salt solution

In Fig. 7(a) the CVs for neat BMPyrrFSI at room temperature (25 ± 1 °C) demonstrate electrochemical stability across a wide range of potentials (up to 4.5 V). The oxidation peak of the gold working electrode surface is seen at E = +1.0 V, with the corresponding reduction peak of gold oxides at E = +0.5 V, indicating the quasi-reversible nature of the Au surface oxidation process. Upon adding 30 mM $Pr(NO_3)_3$ to the BMPyrrFSI IL (close to the saturation limit in the IL at room temperature), no significant reduction peaks of Pr have been observed (Fig.7 a).

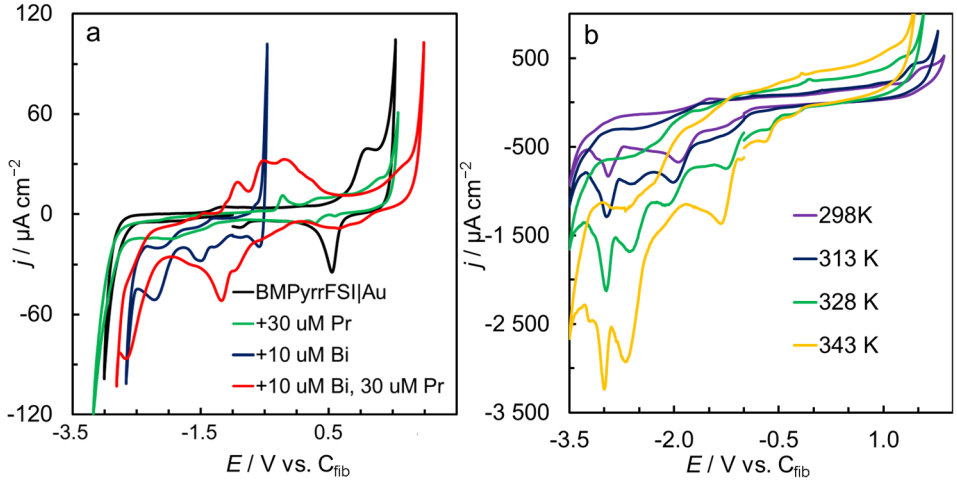

Figure 7. (a) CV curves of polycrystalline Au electrode measured at 298 K in BMPyrrFSI (neat) and with addition of $Bi(OTf)_3$ and $Pr(NO_3)_3$ salts dissolved in BMPyrrFSI; (b) CV curves for BMPyrrFSI with addition of 10 mM $Bi(OTf)_3$ and 30 mM $Pr(NO_3)_3$ measured at different temperatures, noted in Figure.

The reduction peaks at E = –2.0 V; –2.65 V and –3.0 V are likely related to the reduction of Pr^{3+}-ionic liquid anion complexes with different structures (with varying number of anions in the complex or the stepwise reduction of this complex). Thus, the reduction of Pr^{3+} is suggested to occur as a stepwise process when a Bi salt is added to the IL containing Pr^{3+} nitrate. The separation of peaks becomes more pronounced as the temperature and current density increase. The precise mechanism behind this phenomenon requires additional study involving DFT computations and molecular dynamics modeling [108].

Since Pr^{3+} may reduce on Bi layers or previous Pr metallic layers, there are several possibilities that could explain the additional reduction peaks. The increase in temperature significantly increases the reduction rate of Pr^{3+} cations, but it also increases the parasitic Faradaic processes and contributes to the electrochemical breakdown of the IL. Bi can be easily separated by melting out from the Bi-Pr solid deposit through a thermal treatment at a temperature higher than 300º C in a clean N_2 atmosphere.

After CV experiments, EIS measurements were performed to monitor the condition of the interface between Au working electrode and IL. As seen in Fig. 8a, the shape of the Nyquist plot depends on the electrode potential applied. At E = –0.6 V nearly ideal capacitive behavior is observed.

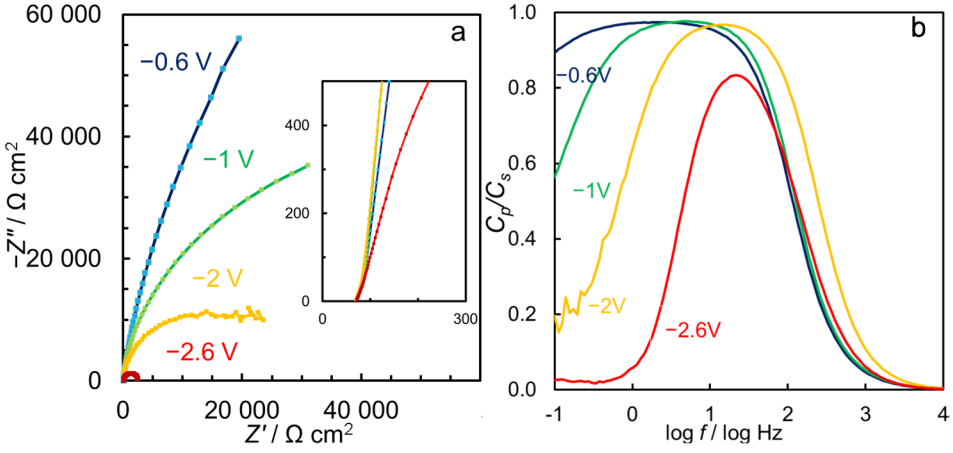

Figure 8. (a) Nyquist plots and (b) frequency dependence of the ratio of parallel capacitance (C_p) to series capacitance (C_s) for Au electrode in the BMPyrrFSI +10 mM $Bi(OTf)_3$+ 30 mM $Pr(NO_3)_3$ system at 298 K (measured at fixed potentials as indicated in the figure).

The Bode phase angle vs log f plots indicate that only at very low AC frequencies, there is some deviation towards mixed kinetics. In an ideally polarizable system, phase angle values equal to –90° must be observed, but at very low frequencies, there is a slight deviation with phase-angle values higher than –90°. At more negative Au electrode potentials, there is a noticeable shift toward mixed kinetics, which involves slow adsorption and slow mass transfer. At E = –1.0 V, the phase-angle values at low-frequencies approach –45º, indicating mixed-kinetic

processes. Lower phase-angle values have been measured at low frequencies at $E = -2.0$ and $E = -2.6$ V, characteristic of slow mass-transfer and Faradaic charge-transfer mixed kinetics as limiting steps. Specifically, this refers to the electro-reduction of Bi^{3+} and Pr^{3+} cations at the Au electrode.

In Fig 8a, the Nyquist plot at $E = -2.6$ V indicates the electroreduction of Bi^{3+} and Pr^{3+} cations at the Au surface. It shows a typical semicircular shape, which is characteristic of mass transfer-limited Faradaic processes. In Fig. 8(b), the ratio of parallel to series capacitance of the Au BMPyrrFSI + 30 mM $Pr(NO_3)_3$ and 10 mM $Bi(OTf)_3$ system is shown. These values are close to unity (>0.95) over a wide frequency and potential range, even at $E = -2$ V, indicating that the Au-IL interface is nearly ideally polarizable over a wide potential range. Only at very low ac frequencies do slow Faradaic processes determine the kinetic behavior of the system under study, as indicated by the low ratio (<0.7) of parallel to series capacitance. At $E = -2.6$ V, the system is limited by mid-frequency mass-transfer and low-frequency charge-transfer processes. This is indicated by the ratio of parallel to series capacitance less than 0.8 and less than 0.1, respectively.

After conducting EIS and CV studies, the Bode phase-angle plot has shifted towards lower frequencies, indicating an increase in the capacitance of the working electrode. This suggests that Bi has formed a layer on the Au electrode, acting as a binding layer and slightly increasing the active surface area of the working electrode due to the very well expressed surface roughness after the the deposition of Bi and Pr [109].

To further investigate, a long lasting study involving the reduction of Pr^{3+} together with Bi^{3+} cations was carried out in chronoamperometric mode for 10 h at fixed constant potential (E = –2.65 V) as shown in Fig. 9.

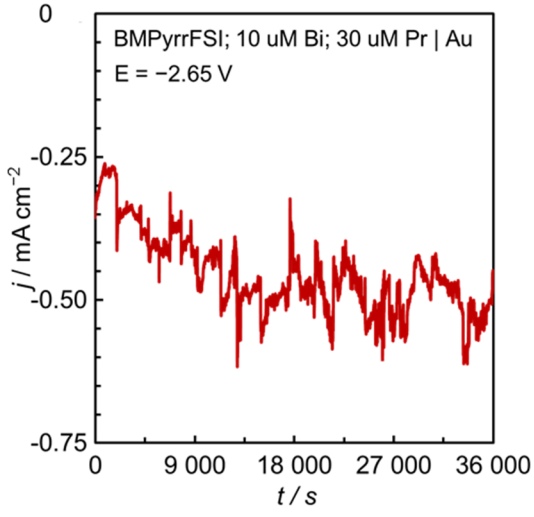

Figure 9. Chronoamperometric curve for the co-reduction of Pr^{3+} and Bi^{3+} at an Au electrode. During deposition, the electrode potential was held constant at E = – 2.65 V vs. a carbon fiber pseudoreference electrode in the same solution , and the temperature was 298 K.

The temperature was maintained at 298 K, and the solution was stirred at 100 rpm to enhance mass transport and accelerate the accumulation of Bi and Pr on the Au electrode surface By reducing the diffusion layer thickness. Throughout the experiment, a cathodic current density ranging from –250 μA/cm^2 (corresponding to only Bi^{3+} reduction) and –600 μA/cm^2 (corresponding to reduction of both Bi^{3+} and Pr^{3+}) was consistently observed, indicating high electrochemical activity. Following the experiment, a dark layer of deposited metals was noticed on the Au working electrode. However, this dark precipitate also detached from the working electrode into the IL solution and settled at to the bottom of the cell. This behavior is also reflected in the jagged lines of the chronoamperometric curve. So, it can be inferred that Bi forms the initial layer on the Au working electrode surface due to its lower electroreduction potential, and subsequently, reduced Pr binds to the Bi layer to some extent. The working electrode surface saw a continuous co-precipitation of Bi and Pr metallic particles. However, because of the mismatch of the lattice constants of Au, Bi and Pr, the polycrystalline Au electrode couldn't consistently bind the reduced metals, causing them to separate from the working electrode surface. As a result, only a small portion of the co-precipitated metals remained on the working electrode surface, and most of the produced materials ended up at the bottom of the electrochemical cell.

Solution with sedimented matter collected from the electrochemical cell was then centrifuged at 5000 rpm in ethanol and washed with deionized water. The results of SEM-EDS analysis of the collected matter are shown in Fig. 10.

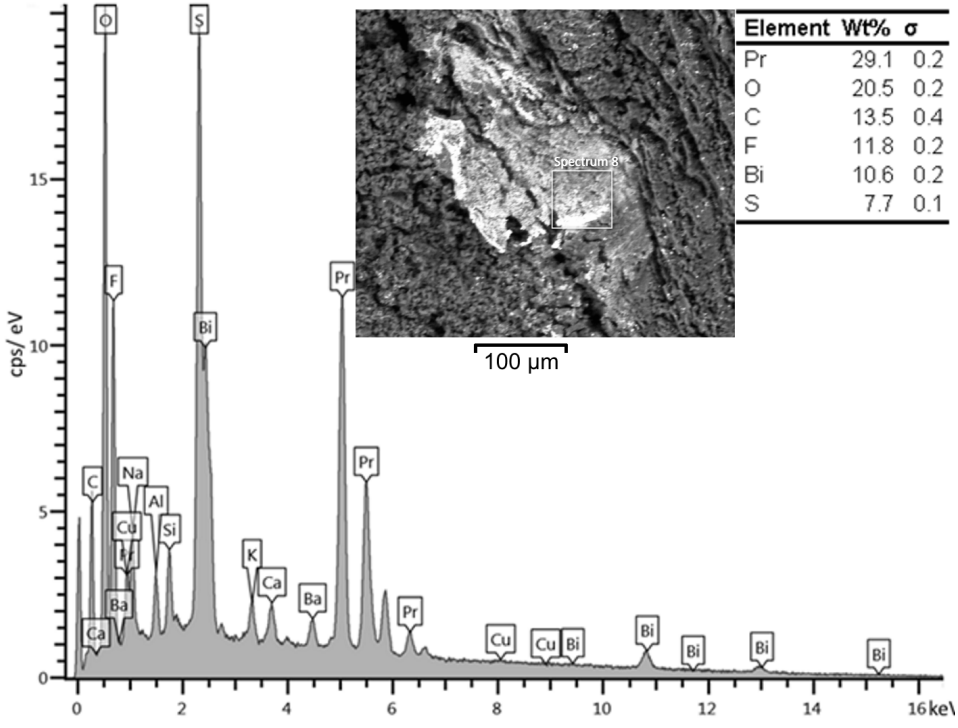

Figure 10. Elemental analysis of the sedimented matter performed by the SEM-EDS method, and SEM picture of the electrode surface after deposition of Bi and Pr.

Pr and Bi were detected, indicating co-precipitation of Bi and Pr. The surface of the working electrode was then rinsed with ethanol, and all precipitated substance was dissolved in concentrated nitric acid for about 10 s until no precipitate was left on the working electrode. The concentrations of Pr in the initial and final solutions of $Pr(NO_3)_3$ and $Bi(OTf)_3$ in BMPyrrFSI were measured. The final solution was vortexed carefully to homogenize it. The concentration of Bi^{3+} was not measured by MP-AES. As seen in Table 1, only 29.25% of Pr^{3+} was left in the final solution. At the same time, only 3.15% of Pr was permanently deposited and thereafter extracted from the working electrode surface with HNO_3 solution. Since reduced Pr can only be found at the working electrode or in the sediment obtained from the bottom of the electrochemical cell, it can be summarized that 67.6% of the Pr is in the sediment at the bottom of the electrochemical cell. In total, 70.75% of the Pr^{3+} was reduced during the electrochemical extraction process. The coulombic efficiency for reducing Pr^{3+} ions has been calculated to be over 80% in experiments conducted at 298 K. The results show that most of the Pr was reduced from Pr^{3+} to the Pr^0 metallic state. However, this only happens when Bi^{3+} is also present in the solution. At the same time, it is clear that the working electrode cannot bind and hold the deposited material. Most of the reduced material fell off the working electrode and precipitated to the bottom of the electrochemical cell. Given that the majority of the Pr falls to the bottom of the cell, it is reasonable to collect the obtained material through centrifugation and additional cleaning. Furthermore, it is still necessary to remove any IL from the final product and to separate Bi from Pr. The remaining Pr^{3+} that has not been deposited can be extracted in the subsequent electrodeposition step after adding a new portion of raw Pr^{3+} solution into the IL. Since metallic praseodymium is not stable in ambient air, the final product would be praseodymium oxide (Pr_2O_3).

6.2.2. Electrochemical separation of yttrium from phosphorite ore

6.2.2.1. Cyclic voltammetry results for concentrated Y and REEs solution

Fig. 11a shows the cyclic voltammograms (CVs) of the electrochemical deposition solution H. It is shown that the electrodeposition of Bi starts at E = –0.8 V and is a reversible process with an oxidation peak at E = –0.6 V corresponding to the stripping of Bi. It is also seen that the electroreduction of Y and other metals starts at significantly lower potentials with an electroreduction peak at E = –2.6 V. Based on our preliminary unpublished results conducted with pure $Y(NO_3)_3$ salt, this results from the electrodeposition on the Y metal and is correlated with the oxidation peak seen at E = –0.3 V, corresponding to the electrostripping of deposited Y.

The electroreduction of HREEs started at E < –2.9V, but this process was not fully studied (the current peak was not fully developed) as the electroreduction process of Y was our main interest at this time. In the CV, the curve scanned toward less negative potentials, and the oxidation of metals started at E= –0.9

to –0.8 V. In addition, the quasi-reversible oxidation peaks between E = –0.9 V to –0.8 V for the oxidation of Bi to Bi^{3+} and at E = –0.4 V for Y to Y^{3+} are relevant to the oxidation of deposited Bi and Y. The data for Bi^{3+} show that there is a normal difference between $E_{ox} - E_{red}$, = 180–200 mV potentials, and thus is characteristic of the 3-electron redox process.

The electro-oxidation process of Y demonstrates a very high difference between the E_{ox}–E_{red} (i.e., very high overvoltage) characteristics of a nearly irreversible process, similar to the results discussed by Bagri et al. [110].

When the electroreduction of the sample is measured below the Bi redox process potential range (Fig. 11a curve 2), significantly higher electrodeposition currents were observed for the electrodeposition of Y below E = –2.2 V. This shows that the electroreduction of Y and other metals from the sample is significantly enhanced without the disturbance of the redox deposition and stripping of the porous Bi adlayer.

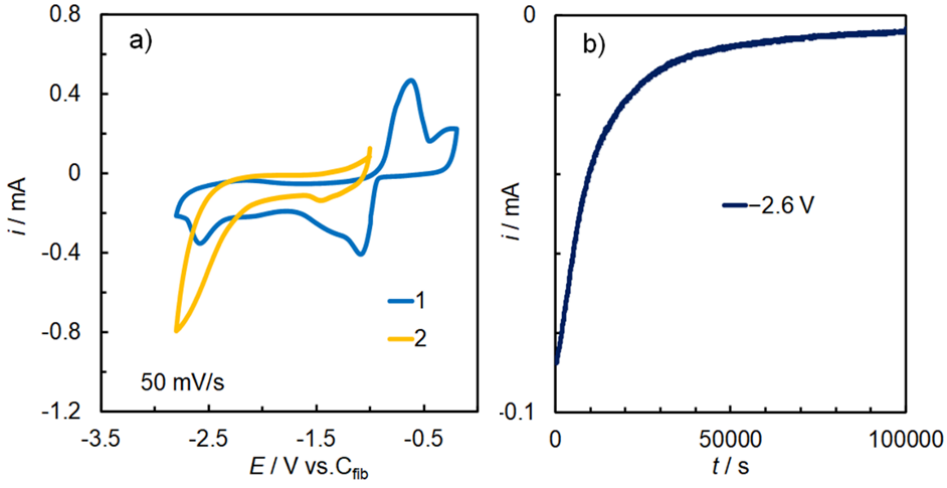

Figure 11. a) Cyclic voltammograms for 0.2 M BMPyrFSI + 50 mM $Bi(OTF)_3$ + PC + REEs extraction solution at potential scanning rate 50 mVs^{-1} in two different potential regions. b) Chronoamperometry data for 0.2 M BMPyrFSI+ 50 mM Bi(OTF)3 +REE extraction solution at E=–2.6 V during 27 h of electrodeposition.

Data in Fig. 11a shows that for an optimized mixture of BMPyrFSI + PC separately containing extracted REEs, (without $Bi(OTF)_3$) the reduction current started to increase only at very negative potential E<–2.2 V. Thus, for precedingly Bi coated Pt electrode (curve 2) the nearly ideal polarizable region was around 2.0 V, in good agreement with data demonstrated in our published paper [30]. There are no very well-developed oxidation peaks for Bi coated Pt electrode in a $Y(NO_3)_3$ containing solution. When examining the CV data for the $Y(NO_3)_3$ dissolved in a mixture of BMPyrFSI + PC + $Bi(OTf)_3$, a distinct reduction peak for Bi^{3+} cations is observed at –1.2 V, along with a less pronounced reduction peak at E = –1.4 V. A well-defined peak is also observed at E = –2.6 V, which

is associated with the reduction of different forms of PC-bound Y^{3+} cations. However, it seems that the low current does not benefit the high efficiency of Y^{3+} electroreduction from the complex natural phosphorite sample with the addition of $Bi(OTF)_3$.

It was found that using a preliminary Bi-modified Pt electrode resulted in higher electroreduction currents for Y^{3+} cations, leading to more efficient reduction of Y^{3+} from extracted Y-REEs nitrate solutions (data in Fig. 11a). Additionally, it was observed that for a quicker and more pronounced electroreduction of Y^{3+}, a higher current can be applied if there is no Bi^{3+} in electrodeposition solution.

It should be noted that the CV for the extracted REE sample dissolved in the IL mixture shows a much higher current (Fig.11a). This high current is not unexpected, as the CV was performed on a Pt electrode coated with Bi and exhibiting very high surface roughness values [48]. The Bi-coated Pt electrode was prepared in a mixture of BMPyrFSI + PC + $Bi(OTf)_3$, and after multiple CV cycles, it displayed an amorphous dark metal layer with high porosity.

After electrodepositing Y onto the Bi-modified Pt electrode, the electrode was removed from the solution at E = –2.0 V and then rinsed with PC to remove dissolved chemicals. The CV result (orange curve in Fig. 11a) was obtained on the newly coated Pt electrode in the mixture of BMPyrFSI + PC + REEs concentrate. The pre-coated bismuth layer not only increases the effective surface area but also solely contributes to the separation process for post-performed Y reduction, as supported by Abdallah *et al*. [109]. When compared with the CV for the pristine sample dissolved in the mixture of BMPyrFSI + PC + $Bi(OTf)_3$ (Fig.12a), the negative potential limit for the extracted sample dissolved in the mixture of BMPyrFSI + PC is detected at a more negative potential due to the decrease in the surface activity of the working electrode (Pt modified with Bi layer) surface activity. This is also the reason why we chose the maximal negative electrodeposition potential of Y at –2.6 V.

6.2.2.2. Chronoamperometry (*i* vs t) results

In section 6.1, it is noted that although the phosphorite ore has a complex chemical composition, extraction and stripping procedures somewhat help to concentrate the Y content from the natural phosphorite sample. Thus, in order to increase the separation efficiency, the final electrodeposition of Y was performed at fixed constant potentials E = –2.0; –2.3; –2.6 for 1 h. The current in the i-t curve (Fig.12b) initially decreased during the first 2500 s. Subsequently, a steady current ranging from –0.06 mA to –0.09 mA was maintained between 2500 s and 3600 s. After 3600 s, there was a sharp current drop, which can be attributed to the rapid depletion of Y^{3+} and REEs cations concentration near the electrode surface. This decrease in surface concentration is due to the quicker electroreduction compared to the stationary mass-transfer rate of cations from the non-stirred solution phase to the electrode surface, i.e., into the reaction zone. A noticeably faster decrease in deposition current was observed for mixtures containing 10 times diluted $Y(NO_3)_3$ and $REE(^{3+})$ cations, as demonstrated in

Fig. 12b. The increase in cathodic current at longer deposition times (t>1600 s) for E = –2.3V compared to data at *E* = –2.0V (Fig.12b) is attributed to the deposition of Bi, Y and other REE metals with more negative redox potential than Bi^{3+}, and Y^{3+}.

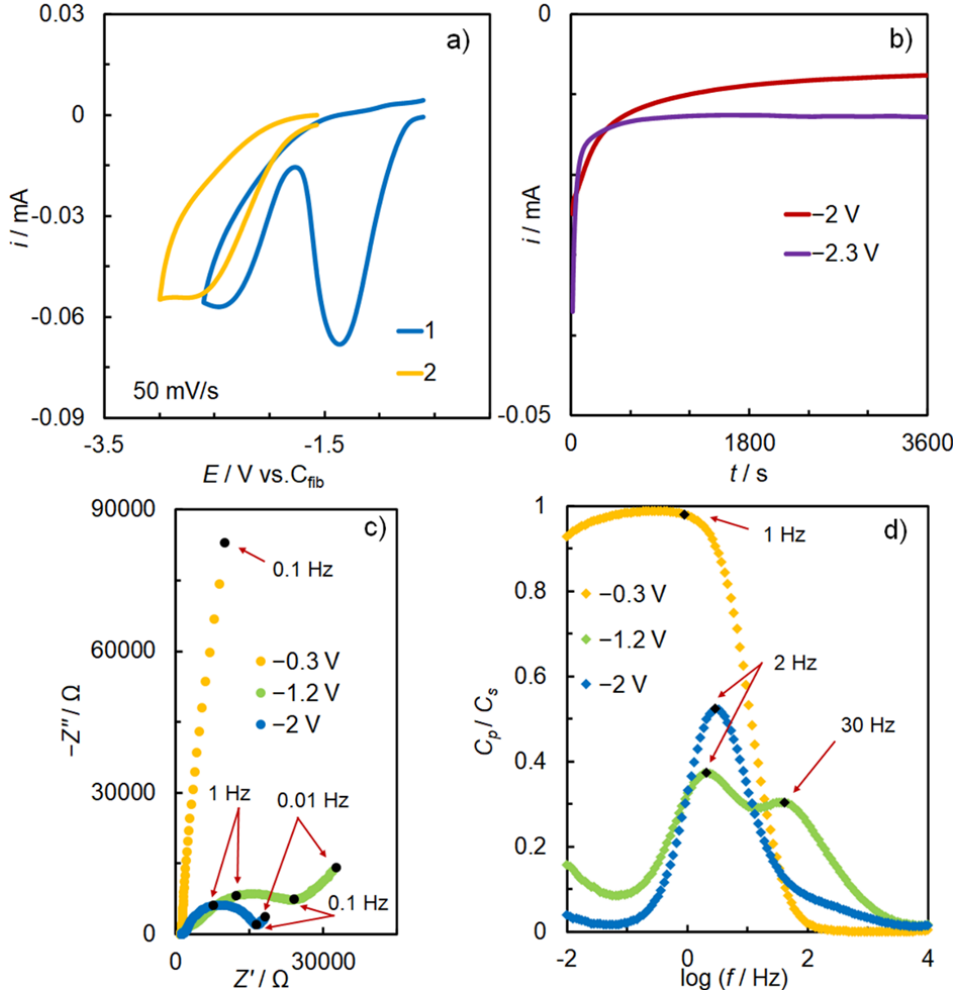

Figure 12. Cyclic voltammetry (*i* vs E) curves at 50 mVs–1 potential scanning rate (a), chronoamperometry (*i* vs t) curves at constant potentials –2.0 V and –2.3V (b), complex impedance plane (Nyquist) plots (c), and the ratio of parallel capacitance (C_p) to series capacitance (C_s) vs. log (frequency) plots at potentials, given in figure (d) for the Pt electrode in 10 mM Bi(OTF)3 + 0.2 M BMPyrFSI in PC with addition of REEs extraction solution.

The working electrode surface initially appears dark sue to a Bi-coating, but a much darker color becomes evident within the first thousand seconds of electro-reduction in RTIL + Y^{3+} + REEs solution. The consistently low current range indicates slow mass-transfer kinetics at the interface. In contrast to our previous article on Bi and Pr co-reduction onto the working electrode surface [28], in some experiments, Y was deposited separately after the completion of the Bi reduction step. It's worth noting that unlike Bi+ Pr deposition, most of the dark precipitate remains on the electrode surface (>70%), a noticeable amount of reduced metals deposits at the bottom of the electrochemical cell (<20%), and only a small portion of Y^{3+} and other REE^{3+} cations can be observed in the electrolyte solution (10%).

6.2.2.3. Impedance analysis

Nyquist (–Z′′ vs Z′) plots presented in Fig 12c and C_p/C_s vs. log *f* plots in Fig.12d show that the electrode potential has noticeable influence on the processes nature and rate limiting processes taking place at Bi modified (electrodeposited) Pt working electrode. At E = –0.3 the shape of Nyquist plot is characteristic of ideally polarizable electrode demonstrating nearly blocking electrode behavior at very low frequencies. At –0.4V <E <–1.2V systematic increase of deviation of system from ideally polarizable interface takes place. At E = –1.2V, two de-pressed semicircles (Fig.12c) at frequencies higher than 0.1Hz, characteristic of slow mixed-kinetics processes (slow adsorption and slow mass-transfer step limited processes) have been established. The first semicircle is very narrow, and it practically disappears with the increase of negative electrode potential. The second semicircle is heavily depressed, and the wideness decreases with the increase of negative potential of Bi covered electrode. At very low frequencies the nearly linear areas with the nearly 45 degrees slope. characteristic of the mass-transfer limited step processes can be seen. The C_p/C_s vs. log f plots shape, demonstrated in Fig 12d, very noticeably depends on E applied. At E = –0.3 V nearly ideally polarizable behavior has been observed. At E = –1.2 V, the curve with two maxima has been observed. The first peak at 100Hz corresponds to the mixed kinetic mas-transfer and charge transfer process and maximum at 3–5 Hz is characteristic of mixed kinetic process connected with slow mass-transfer step inside of porous Bi layer with very high surface roughness, studied already by Romann et al.[111], because the E is not so negative needed for electroreduction/ deposition of Y at electrode surface. At lower frequencies the very slow mass-transfer and charge transfer limited processes with phase angle value –22.5 degree have been observed. With the increase of negative potential value from E= –1.6V to E = –2.0V systematic shift of processes toward mixed charge transfer and mass-transfer processes takes place. At E = –2.0 V, the Nyquist plot (Fig.12c) and C_p/C_s vs. log f plots shape (Figs 12d) is controlled by the slow mixed kinetic charge transfer at high frequencies, but at lower frequencies the typical mixed kinetic behavior with slow mass-transfer and charge transfer kinetics (up to f<0.1 Hz) takes place.

6.2.2.4. Selectivity experiments

From the selectivity experiments, it was shown that $E < -2.0$ V is required for Y deposition. Thus, many additional elements, such as Fe (>90%), Cu (>85%), Mn (>90%), Zn (>80%), and, importantly, Sr (>95%), will be deposited prior to Y at $E = -2.0$ V during 4 h. This means that fewer chemical purification steps will be necessary when electrodeposition is conducted in multiple steps.

Our previous studies [30] indicate that bismuth plays an important role in the electrochemical reduction process of REEs electroreduction. Bismuth reduction from Bi^{3+} cation to a zero-valence metallic state occurs at a less negative potential, forming the first layer at the Pt electrode's surface and acting as a binder for the other metals that are reduced and deposited onto the Bi-modified electrode surface. The experiment results with praseodymium trinitrate salt, along with $Bi(OTf)_3$ in ionic liquid electrolyte, indicated that a reduction of the Pr3+ cation only occurs if the Bi^{3+} cation is present. Hence, the formation of a Bi-Pr bimetallic layer was suggested [28]. But differently from Pr^{3+} reduction, when considering Y^{3+} reduction, the position Y(0) does not delaminate from the Bi-modified Pt electrode's surface. However, after electroreduction, many other REEs delaminated from the Bi(0)-modified electrode's surface, exhibiting a very high surface roughness [30] and porosity with a very amorphous and soft structure.

7. SUMMARY

A two-step extraction method for the separation at first of U, Th, Tl, and then all rare earth elements from the phosphorite ore has been developed using tri-n-octylmethylammonium nitrate noted as A336[NO_3]) and bis(2-ethylhexyl) phosphate (D2EHPA) as the extractants. The extraction efficiency for radioactive elements and all REEs with D2EHPA from concentrated nitric acid and partly neutralized nitric acid media was found to be very high. Based upon the solvent extraction studies, dry examples of extracted concentrated phosphorite ore have been obtained and used further in electrochemical extraction experiments.

It has been demonstrated that praseodymium metal can be electrochemically deposited onto a gold working electrode from praseodymium trinitrate solution in RTIL if Bi^{3+} cations are added to the mixture. The cyclic voltammetry data shows two cathodic peaks for praseodymium cation electroreduction at $E = -1.25$ and –2.6 V, indicating the electroreduction of Pr^{3+} to Pr^0. This reduction likely occurs through stepwise stabilized intermediate oxidation states. Around 70% of the reduced praseodymium precipitated from the initial solution of $Pr(NO_3)_3$ and $Bi(OTf)_3$ in BMPyrrFSI after a 10-hour electrolysis in chronoamperometric mode.

Electrochemical deposition of Y from the Estonian Ülgase phosphorite ore concentrated sample has been demonstrated. After the preliminary liquid extraction Y was successfully deposited onto a Bi modified platinum working electrode at $E = -2.6$ V. Before Y or REEs can be electrochemically deposited, B-group metals and Sr can be extracted from the solution by electrochemical deposition at $E = -2$ V. It was shown that this extraction method can be highly efficient as well as selective when well-controlled different electrodeposition conditions are applied.

8. REFERENCES

[1] K. Guzik, K. Galos, A. Kot-Niewiadomska, T. Eerola, P. Eilu, J. Carvalho, F.J. Fernandez-Naranjo, R. Arvidsson, N. Arvanitidis, A. Raaness, Potential benefits and constraints of development of critical raw materials' production in the EU: Analysis of selected case studies, Resources 10 (2021) 67.

[2] V. Balaram, Potential Future Alternative Resources for Rare Earth Elements: Opportunities and Challenges, Minerals 13 (2023) 425. https://doi.org/10.3390/min13030425.

[3] W. Gao, D. Wen, J.C. Ho, Y. Qu, Incorporation of rare earth elements with transition metal–based materials for electrocatalysis: a review for recent progress, Materials Today Chemistry 12 (2019) 266–281. https://doi.org/10.1016/j.mtchem.2019.02.002.

[4] S. Tian, L. Zhang, R. Xie, A. Lu, Y. Huang, H. Xing, X. Chen, The electronic, magnetic and optical properties of GaN monolayer doped with rare-earth elements, Solid State Communications 371 (2023) 115292. https://doi.org/10.1016/j.ssc.2023.115292.

[5] P. Long, Y. Qiuhui, H. Zhang, X.U. Guangliang, M. Zhang, W. Jingdong, Rare earth permanent magnets Sm2 (Co, Fe, Cu, Zr) 17 for high temperature applications, Journal of Rare Earths 26 (2008) 378–382.

[6] S. Qiao, Q. Zhou, M. Ma, H.K. Liu, S.X. Dou, S. Chong, Advanced Anode Materials for Rechargeable Sodium-Ion Batteries, ACS Nano 17 (2023) 11220–11252. https://doi.org/10.1021/acsnano.3c02892.

[7] H. Zhao, J. Xia, D. Yin, M. Luo, C. Yan, Y. Du, Rare earth incorporated electrode materials for advanced energy storage, Coordination Chemistry Reviews 390 (2019) 32–49. https://doi.org/10.1016/j.ccr.2019.03.011.

[8] A. Ringuedé, S. Hubert, L. Atwi, V. Lair, Prospects of hydrogen and its derivative as energy vector for electricity production at high temperature: Fuel cells and electrolysers, Current Opinion in Electrochemistry 42 (2023) 101401. https://doi.org/10.1016/j.coelec.2023.101401.

[9] M. Vestli, E. Lust, G. Nurk, Characterization of Terbium and Samarium Co-Doped Ceria Films Prepared Using Ultrasonic Spray Pyrolysis, J. Electrochem. Soc. 162 (2015) F812–F820. https://doi.org/10.1149/2.0031508jes.

[10] E. Lust, P. Möller, I. Kivi, G. Nurk, S. Kallip, P. Nigu, K. Lust, Optimization of the cathode composition for the intermediate-temperature SOFC, Journal of the Electrochemical Society 152 (2005) A2306.

[11] U. Ryszko, P. Rusek, D. Kołodyńska, Quality of Phosphate Rocks from Various Deposits Used in Wet Phosphoric Acid and P-Fertilizer Production, Materials 16 (2023) 793. https://doi.org/10.3390/ma16020793.

[12] K. Binnemans, P.T. Jones, B. Blanpain, T. Van Gerven, Y. Pontikes, Towards zero-waste valorisation of rare-earth-containing industrial process residues: a critical review, Journal of Cleaner Production 99 (2015) 17–38. https://doi.org/10.1016/j.jclepro.2015.02.089.

[13] S. Riaño, K. Binnemans, Extraction and separation of neodymium and dysprosium from used NdFeB magnets: an application of ionic liquids in solvent extraction towards the recycling of magnets, Green Chemistry 17 (2015) 2931–2942. https://doi.org/10.1039/C5GC00230C.

[14] F.J. Alguacil, J.I. Robla, Recent Work on the Recovery of Rare Earths Using Ionic Liquids and Deep Eutectic Solvents, Minerals 13 (2023) 1288. https://doi.org/10.3390/min13101288.
[15] I. Komasawa, K. Hisada, M. Miyamura, Extraction and separation of rare-earth elements by tri-n-octylmethylammonium nitrate, Journal of Chemical Engineering of Japan 23 (1990) 308–315.
[16] A. Rout, K. Binnemans, Separation of rare earths from transition metals by liquid–liquid extraction from a molten salt hydrate to an ionic liquid phase, Dalton Trans. 43 (2014) 3186–3195. https://doi.org/10.1039/C3DT52541D.
[17] A. Kumari, K.K. Sahu, S.K. Sahu, Solvent Extraction and Separation of Nd, Pr and Dy from Leach Liquor of Waste NdFeB Magnet Using the Nitrate Form of Mextral® 336At in the Presence of Aquo-Complexing Agent EDTA, Metals 9 (2019) 269. https://doi.org/10.3390/met9020269.
[18] K. Larsson, K. Binnemans, Separation of Rare Earths by Solvent Extraction with an Undiluted Nitrate Ionic Liquid, Journal of Sustainable Metallurgy 3 (2017) 73–78. https://doi.org/10.1007/s40831-016-0074-4.
[19] H. Liang, P. Zhang, Z. Jin, D.W. DePaoli, Rare earth and phosphorus leaching from a flotation tailings of florida phosphate rock, Minerals 8 (2018) 416.
[20] H. Liang, P. Zhang, Z. Jin, D. DePaoli, Rare Earth and Phosphorus Leaching from a Flotation Tailings of Florida Phosphate Rock, Minerals 8 (2018) 416. https://doi.org/10.3390/min8090416.
[21] J.I. Skorovarov, V.D. Kosynkin, S.D. Moiseev, N.N. Rura, Recovery of rare earth elements from phosphorites in the USSR, Journal of Alloys and Compounds 180 (1992) 71–76. https://doi.org/10.1016/0925-8388(92)90364-F.
[22] S.B. Castor, Rare Earth Deposits of North America, Resource Geology 58 (2008) 337–347. https://doi.org/10.1111/j.1751-3928.2008.00068.x.
[23] M. Chen, T.E. Graedel, The potential for mining trace elements from phosphate rock, Journal of Cleaner Production 91 (2015) 337–346. https://doi.org/10.1016/j.jclepro.2014.12.042.
[24] W. Chen, F. Zhou, H. Wang, S. Zhou, C. Yan, The Occurrence States of Rare Earth Elements Bearing Phosphorite Ores and Rare Earth Enrichment Through the Selective Reverse Flotation, Minerals 9 (2019) 698. https://doi.org/10.3390/min9110698.
[25] S.-H. Yin, S.-W. Li, W.-Y. Wu, X. Bian, J.-H. Peng, L.-B. Zhang, Extraction and separation of Ce(III) and Pr(III) in the system containing two complexing agents with di- (2-ethylhexyl) phosphoric acid, RSC Adv. 4 (2014) 59997–60001. https://doi.org/10.1039/C4RA10143J.
[26] S. Rout, Abhilash, P. Meshram, P. Zhang, A Comprehensive Review on Occurrence and Processing of Phosphate Rock Based Resources-Focus on REEs, Mineral Processing and Extractive Metallurgy Review 45 (2024) 368–388. https://doi.org/10.1080/08827508.2022.2161537.
[27] S. Wu, L. Zhao, L. Wang, X. Huang, Y. Zhang, Z. Feng, D. Cui, Simultaneous recovery of rare earth elements and phosphorus from phosphate rock by phosphoric acid leaching and selective precipitation: Towards green process, Journal of Rare Earths 37 (2019) 652–658. https://doi.org/10.1016/j.jre.2018.09.012.
[28] S. Wu, L. Wang, L. Zhao, P. Zhang, H. El-Shall, B. Moudgil, X. Huang, L. Zhang, Recovery of rare earth elements from phosphate rock by hydrometallurgical processes – A critical review, Chemical Engineering Journal 335 (2018) 774–800. https://doi.org/10.1016/j.cej.2017.10.143.

[29] S. Jürjo, L. Siinor, C. Siimenson, P. Paiste, E. Lust, Two-Step Solvent Extraction of Radioactive Elements and Rare Earths from Estonian Phosphorite Ore Using Nitrated Aliquat 336 and Bis(2-ethylhexyl) Phosphate, Minerals 11 (2021) 388. https://doi.org/10.3390/min11040388.
[30] S. Jürjo, O. Oll, P. Paiste, M. Külaviir, J. Zhao, E. Lust, Electrochemical co-reduction of praseodymium and bismuth from 1-butyl-1-methylpyrrolidinium bis (fluorosulfonyl) imide ionic liquid, Electrochemistry Communications 138 (2022) 107285.
[31] S. Ni, Y. Gao, G. Yu, S. Zhang, Z. Zeng, X. Sun, Tailored ternary hydrophobic deep eutectic solvents for synergistic separation of yttrium from heavy rare earth elements, Green Chemistry 24 (2022) 7148–7161.
[32] H. Su, S. Ni, C. Bie, S. Wu, X. Sun, Efficient and sustainable separation of yttrium from heavy rare earth using functionalized ionic liquid [N1888][NDA], Separation and Purification Technology 285 (2022) 120302.
[33] V. Agarwal, M.S. Safarzadeh, J. Galvin, Solvent extraction and separation of Y (III) from sulfate, nitrate and chloride solutions using PC88A diluted in kerosene, Mineral Processing and Extractive Metallurgy Review 39 (2018) 258–265.
[34] Y. Wang, H. Zhou, Y. Wang, F. Li, X. Sun, Separation of high-purity yttrium from ion-absorbed rare earth concentrate using (2, 6-dimethylheptyl) phenoxy acetic/ propanoic acid, Separation and Purification Technology 184 (2017) 280–287.
[35] T. Miaomiao, J.I.A. Qiong, L. Wuping, Studies on synergistic solvent extraction of rare earth elements from nitrate medium by mixtures of 8-hydroxyquinoline with Cyanex 301 or Cyanex 302, Journal of Rare Earths 31 (2013) 604–608.
[36] N.K. Batchu, B. Dewulf, S. Riaño, K. Binnemans, Development of a solvo-metallurgical process for the separation of yttrium and europium by Cyanex 923 from ethylene glycol solutions, Separation and Purification Technology 235 (2020) 116193.
[37] D.J. Sapsford, R.J. Bowell, J.N. Geroni, K.M. Penman, M. Dey, Factors influencing the release rate of uranium, thorium, yttrium and rare earth elements from a low grade ore, Minerals Engineering 39 (2012) 165–172.
[38] V. Vukojević, S. \DJur\djić, V. Stefanović, J. Trifković, D. Čakmak, V. Perović, J. Mutić, Scandium, yttrium, and lanthanide contents in soil from Serbia and their accumulation in the mushroom Macrolepiota procera (Scop.) Singer, Environmental Science and Pollution Research 26 (2019) 5422–5434.
[39] H. Chen, L. Chen, L. Zhang, M. Guo, Spatial Heterogeneity of Rare Earth Elements: Implications for the Topsoil of Regional Ion-Adsorption Type Rare Earth Deposit Areas in Southern China, Minerals 13 (2023) 784. https://doi.org/10.3390/min13060784.
[40] M. Kovarikova, I. Tomaskova, P. Soudek, Rare earth elements in plants, Biologia Plantarum 63 (2019) 20–32. https://doi.org/10.32615/bp.2019.003.
[41] J.P. Hallett, T. Welton, Room-Temperature Ionic Liquids: Solvents for Synthesis and Catalysis. 2, Chem. Rev. 111 (2011) 3508–3576. https://doi.org/10.1021/cr1003248.
[42] A. Abbott, M. Addicoat, L. Aldous, R.G. Bhuin, N. Borisenko, J.N.C. Lopes, R. Clark, S. Coles, M.C. Gomes, B. Cross, J. Everts, M. Firestone, R. Gardas, M. Gras, S. Halstead, C. Hardacre, J. Holbrey, T. Itoh, V. Ivaništšev, J. Jacquemin, P. Jessop, R. Jones, B. Kirchner, S. Li, R. Lynden-Bell, D. MacFarlane, F. Maier, M. Mezger, A. Pádua, O.D. Pavel, S. Perkin, S. Purcell, M. Rutland, J.M. Slattery, S. Suzer, K. Tamura, M.L. Thomas, S. Tiwari, S. Tsuzuki, B. Uralcan, W. Wallace,

M. Watanabe, J. Wishart, Ionic liquids at interfaces: general discussion, Faraday Discuss. 206 (2017) 549–586. https://doi.org/10.1039/C7FD90094E.
[43] M. Amde, J.-F. Liu, L. Pang, Environmental application, fate, effects, and concerns of ionic liquids: a review, Environ. Sci. Technol 49 (2015) 12611–12627.
[44] M.L. Dietz, Ionic Liquids as Extraction Solvents: Where do We Stand?, Separation Science and Technology 41 (2006) 2047–2063. https://doi.org/10.1080/01496390600743144.
[45] A.P. Abbott, G. Frisch, K.S. Ryder, Electroplating using ionic liquids, Annu. Rev. Mater. Res. 43 (2013) 335–358. https://doi.org/10.1146/annurev-matsci-071312-121640.
[46] R. Böttcher, S. Mai, A. Ispas, A. Bund, Aluminum Deposition and Dissolution in [EMIm]Cl-Based Ionic Liquids–Kinetics of Charge–Transfer and the Rate–Determining Step, J. Electrochem. Soc. 167 (2020) 102516.
[47] X. Jiang, R. Qiao, Electrokinetic Transport in Room-Temperature Ionic Liquids: Amplification by Short-Wavelength Hydrodynamics, J. Phys. Chem. C 116 (2012) 1133–1138. https://doi.org/10.1021/jp2102594.
[48] J. Zhao, G. Gorbatovski, O. Oll, E. Anderson, E. Lust, Influence of water on the electrochemical characteristics and nanostructure of Bi(hkl) │ Ionic liquid interface, Electrochimica Acta 415 (2022) 140263. https://doi.org/10.1016/j.electacta.2022.140263.
[49] J. Zhao, G. Gorbatovski, O. Oll, T. Thomberg, E. Lust, Effect of alkali and halide ion doping on the energy storage characteristics of ionic liquid based supercapacitors, Electrochim. Acta 319 (2019) 82–87. https://doi.org/10.1016/j.electacta.2019.06.176.
[50] H. Ota, M. Matsumiya, N. Sasaya, K. Nishihata, K. Tsunashima, Investigation of electrodeposition behavior for Nd(III) in [P2225][TFSA] ionic liquid by EQCM methods with elevated temperatures, Electrochimica Acta 222 (2016) 20–26. https://doi.org/10.1016/j.electacta.2016.11.038.
[51] C.A. Angell, Y. Ansari, Z. Zhao, Ionic liquids: past, present and future, Faraday Discuss. 154 (2011) 9–27. https://doi.org/10.1039/C1FD00112D.
[52] M. Yamagata, Y. Katayama, T. Miura, Electrochemical behavior of samarium, europium, and ytterbium in hydrophobic room-temperature molten salt systems, J. Electrochem. Soc. 153 (2006) E5. https://doi.org/10.1149/1.2136088.
[53] L.M. Glukhov, A.A. Greish, L.M. Kustov, Electrodeposition of rare earth metals Y, Gd, Yb in ionic liquids, Russ. J. Phys. Chem. 84 (2010) 104–108. https://doi.org/10.1134/S0036024410010206.
[54] E. Bourbos, I. Giannopoulou, A. Karantonis, I. Paspaliaris, D. Panias, Reduction of light rare earths and a proposed process for Nd electrorecovery based on ionic liquids, J. Sustain. Metall. 4 (2018) 395–406. https://doi.org/10.1007/s40831-018-0186-0.
[55] S. Legeai, S. Diliberto, N. Stein, C. Boulanger, J. Estager, N. Papaiconomou, M. Draye, Room-temperature ionic liquid for lanthanum electrodeposition, Electrochemistry Communications 10 (2008) 1661–1664. https://doi.org/10.1016/j.elecom.2008.08.005.
[56] S. Murakami, M. Matsumiya, T. Yamada, K. Tsunashima, Extraction of Pr(III), Nd(III), and Dy(III) from HTFSA aqueous solution by TODGA/phosphonium-based ionic liquids, Solvent Extraction and Ion Exchange 34 (2016) 172–187. https://doi.org/10.1080/07366299.2016.1144951.

[57] O. Borodin, J. Vatamanu, G. Smith, Bulk and Interfacial Behavior of Ionic Liquids from Molecular Dynamics Simulations, ECS. Trans. 33 (2010) 583–599.
[58] Y. Chen, S. Liu, Z. Bi, Z. Li, F. Zhou, R. Shi, T. Mu, Reviewing electrochemical stability of ionic liquids-/deep eutectic solvents-based electrolytes in lithium-ion, lithium-metal and post-lithium-ion batteries for green and safe energy, Green Energy Environ. (2023). https://doi.org/10.1016/j.gee.2023.05.002.
[59] R. Raudsep, Estonian georesources in the European context, Estonian Journal of Earth Sciences 57 (2008) 80. https://doi.org/10.3176/earth.2008.2.03.
[60] K.T. Basuki, A. Rohmaniyyah, W.R. Pusparini, A. Saputra, Extraction development for the separation of gadolinium from yttrium and dysprosium concentrate in nitric acid using cyanex 572, Extraction 11 (2020).
[61] E.A. Puzikov, B.Y. Zilberman, N.D. Goletskii, A.S. Kudinov, Description of the Extraction of Rare Earth Element Nitrates from Weakly Acidic Solutions with Concentrated Tributyl Phosphate Solutions, Radiochemistry 61 (2019) 447–458.
[62] C. Erust, M.K. Karacahan, T. Uysal, Hydrometallurgical Roadmaps and Future Strategies for Recovery of Rare Earth Elements, Mineral Processing and Extractive Metallurgy Review 44 (2023) 436–450. https://doi.org/10.1080/08827508.2022.2073591.
[63] L. Jia, J. Huang, Z. Ma, X. Liu, X. Chen, J. Li, L. He, Z. Zhao, Research and development trends of hydrometallurgy: An overview based on Hydrometallurgy literature from 1975 to 2019, Transactions of Nonferrous Metals Society of China 30 (2020) 3147–3160. https://doi.org/10.1016/S1003-6326(20)65450-4.
[64] Z. Zhu, Y. Pranolo, C.Y. Cheng, Separation of uranium and thorium from rare earths for rare earth production – A review, Minerals Engineering 77 (2015) 185–196. https://doi.org/10.1016/j.mineng.2015.03.012.
[65] S. Wu, L. Wang, L. Zhao, P. Zhang, H. El-Shall, B. Moudgil, X. Huang, L. Zhang, Recovery of rare earth elements from phosphate rock by hydrometallurgical processes – A critical review, Chemical Engineering Journal 335 (2018) 774–800.
[66] S. Wu, L. Wang, P. Zhang, H. El-Shall, B. Moudgil, X. Huang, L. Zhao, L. Zhang, Z. Feng, Simultaneous recovery of rare earths and uranium from wet process phosphoric acid using solvent extraction with D2EHPA, Hydrometallurgy 175 (2018) 109–116. https://doi.org/10.1016/j.hydromet.2017.10.025.
[67] F. Habashi, The recovery of the lanthanides from phosphate rock, Journal of Chemical Technology and Biotechnology. Chemical Technology 35 (1985) 5–14.
[68] F. Xie, T.A. Zhang, D. Dreisinger, F. Doyle, A critical review on solvent extraction of rare earths from aqueous solutions, Minerals Engineering 56 (2014) 10–28. https://doi.org/10.1016/j.mineng.2013.10.021.
[69] M. Nascimento, B.M. Valverde, F.A. Ferreira, R.D.C. Gomes, P.S.M. Soares, Separation of rare earths by solvent extraction using DEHPA, Rem: Rev. Esc. Minas 68 (2015) 427–434. https://doi.org/10.1590/0370-44672015680140.
[70] J.R. Kumar, J.-S. Kim, J.-Y. Lee, H.-S. Yoon, A Brief Review on Solvent Extraction of Uranium from Acidic Solutions, Separation & Purification Reviews 40 (2011) 77–125. https://doi.org/10.1080/15422119.2010.549760.
[71] Y. Zhang, Z. Liu, F. Fan, L. Zhu, Y. Shen, Extraction of Uranium and Thorium from Nitric Acid Solution by TODGA in Ionic Liquids, Separation Science and Technology 49 (2014) 1895–1902. https://doi.org/10.1080/01496395.2014.903279.

[72] B. Gupta, P. Malik, A. Deep, Extraction of uranium, thorium and lanthanides using Cyanex-923: Their separations and recovery from monazite, Journal of Radioanalytical and Nuclear Chemistry 251 (2002) 451–456. https://doi.org/10.1023/A:1014890427073.
[73] S. Jürjo, O. Oll, E. Lust, Yttrium Separation from Phosphorite Extract Using Liquid Extraction with Room Temperature Ionic Liquids Followed by Electrochemical Reduction, Metals 14 (2024) 927. https://doi.org/10.3390/met14080927.
[74] H. Matsuura, H. Numata, R. Fujita, H. Akatsuka, Reprocessing of spent hydrogen absorbing alloys by using electrochemical techniques in molten salts, Journal of Physics and Chemistry of Solids 66 (2005) 439–442. https://doi.org/10.1016/j.jpcs.2004.06.091.
[75] Z. Li, D. Tang, S. Meng, L. Gu, Y. Dai, Z. Liu, Electrolytic separation of Dy from Sm in molten LiCl-KCl using Pb-Bi eutectic alloy cathode, Separation and Purification Technology 276 (2021) 119045. https://doi.org/10.1016/j.seppur.2021.119045.
[76] B. Holcombe, N. Sinclair, R. Wasalathanthri, B. Mainali, E. Guarr, A.A. Baker, S.O. Usman, E. Kim, S. Sen-Britain, H. Jin, S.K. McCall, R. Akolkar, Sustainable and Energy-Efficient Production of Rare-Earth Metals via Chloride-Based Molten Salt Electrolysis, ACS Sustainable Chem. Eng. 12 (2024) 4186–4193. https://doi.org/10.1021/acssuschemeng.3c07720.
[77] J. Zhou, X. Meng, R. Zhang, H. Liu, Z. Liu, Progress on electrodeposition of rare earth metals and their alloys, Electrocatalysis 12 (2021) 628–640. https://doi.org/10.1007/s12678-021-00688-1.
[78] T. Tsuda, C.L. Hussey, Electrochemistry of room-temperature ionic liquids and melts, in: R.E. White (Ed.), Modern Aspects of Electrochemistry, No. 45, Springer New York, New York, NY, 2009: pp. 63–174. https://doi.org/10.1007/978-1-4419-0655-7_2.
[79] M. Galinski, A. Lewandowski, I. Stepniak, Ionic liquids as electrolytes, Electrochim. Acta 51 (2006) 5567–5580. https://doi.org/10.1016/j.electacta.2006.03.016.
[80] E. Quijada-Maldonado, F. Olea, R. Sepúlveda, J. Castillo, R. Cabezas, G. Merlet, J. Romero, Possibilities and challenges for ionic liquids in hydrometallurgy, Separation and Purification Technology 251 (2020) 117289. https://doi.org/10.1016/j.seppur.2020.117289.
[81] C. Aliaga, C.S. Santos, S. Baldelli, Surface chemistry of room-temperature ionic liquids, Phys. Chem. Chem. Phys. 9 (2007) 3683–3700.
[82] M. Hayyan, F.S. Mjalli, M.A. Hashim, I.M. AlNashef, T.X. Mei, Investigating the electrochemical windows of ionic liquids, J. Ind. Eng. Chem. 19 (2013) 106–112. https://doi.org/10.1016/j.jiec.2012.07.011.
[83] A.A. Aal, R. Al-Salman, M. Al-Zoubi, N. Borissenko, F. Endres, O. Höfft, A. Prowald, S. Zein El Abedin, Interfacial electrochemistry and electrodeposition from some ionic liquids: In situ scanning tunneling microscopy, plasma electrochemistry, selenium and macroporous materials, Electrochim. Acta 56 (2011) 10295–10305. https://doi.org/10.1016/j.electacta.2011.02.063.
[84] C. Yan, H. Yi-xin, L. Yan, Applications of ionic liquids in electrodeposition of rare earths *, (2010) 10.

[85] E. Bourbos, I. Giannopoulou, A. Karantonis, I. Paspaliaris, D. Panias, Chapter 13 – Electrodeposition of Rare Earth Metals from Ionic Liquids, in: I.B.D. Lima, W.L. Filho (Eds.), Rare Earths Industry, Elsevier, Boston, 2016: pp. 199–207. https://doi.org/10.1016/B978-0-12-802328-0.00013-9.
[86] A.P. Abbott, F. Qiu, H.M.A. Abood, M.R. Ali, K.S. Ryder, Double layer, diluent and anode effects upon the electrodeposition of aluminium from chloroaluminate based ionic liquids, Phys. Chem. Chem. Phys. 12 (2010) 1862–1872. https://doi.org/10.1039/b917351j.
[87] F. Endres, D. MacFarlane, A. Abbott, Electrodeposition from Ionic Liquids, John Wiley & Sons, 2008.
[88] Y. Castrillejo, M.R. Bermejo, P. Díaz Arocas, A.M. Martínez, E. Barrado, Electrochemical behaviour of praseodymium (III) in molten chlorides, Journal of Electroanalytical Chemistry 575 (2005) 61–74. https://doi.org/10.1016/j.jelechem.2004.08.020.
[89] L. Coustan, G. Shul, D. Bélanger, Electrochemical behavior of platinum, gold and glassy carbon electrodes in water-in-salt electrolyte, Electrochemistry Communications 77 (2017) 89–92. https://doi.org/10.1016/j.elecom.2017.03.001.
[90] M.H. Joo, S.J. Park, S.M. Hong, C.K. Rhee, Y. Sohn, Electrochemical Recovery and Behaviors of Rare Earth (La, Ce, Pr, Nd, Sm, Eu, Gd, Tb, Dy, Ho, Er, Tm, and Yb) Ions on Ni Sheets, Materials 13 (2020) 5314. https://doi.org/10.3390/ma13235314.
[91] W. Zhang, A. Li, H. Chen, B. Lan, K. Pan, T. Zhang, M. Fang, S. Liu, W. Zhang, The effect of rare earth metals on the microstructure and electrochemical corrosion behavior of lead calcium grid alloys in sulfuric acid solution, Journal of Power Sources 203 (2012) 145–152. https://doi.org/10.1016/j.jpowsour.2011.11.067.
[92] A.J. Bard, L.R. Faulkner, Electrochemical methods: fundamentals and applications, Wiley, New York, 2001.
[93] V. Balaram, Rare earth elements: A review of applications, occurrence, exploration, analysis, recycling, and environmental impact, Geoscience Frontiers 10 (2019) 1285–1303. https://doi.org/10.1016/j.gsf.2018.12.005.
[94] E. Barsoukov, J.R. Macdonald, Impedance spectroscopy: theory, experiment, and applications, Wiley, John & Sons, Incorporated, Hoboken, New Jersey, 2005.
[95] R. Väli, A. Jänes, E. Lust, Alkali-Metal Insertion Processes on Nanospheric Hard Carbon Electrodes: An Electrochemical Impedance Spectroscopy Study, J. Electrochem. Soc. 164 (2017) E3429–E3437. https://doi.org/10.1149/2.0431711jes.
[96] M.D. Murbach, D.T. Schwartz, Analysis of Li-Ion Battery Electrochemical Impedance Spectroscopy Data: An Easy-to-Implement Approach for Physics-Based Parameter Estimation Using an Open-Source Tool, J. Electrochem. Soc. 165 (2018) A297–A304. https://doi.org/10.1149/2.1021802jes.
[97] R.M. Torresi, L. Lodovico, T.M. Benedetti, M.R. Alcântara, C. Debiemme-Chouvy, C. Deslouis, Convective mass transport in ionic liquids studied by electrochemical and electrohydrodynamic impedance spectroscopy, Electrochimica Acta 93 (2013) 32–43. https://doi.org/10.1016/j.electacta.2013.01.050.
[98] C. Désilets, A. Lasia, Dynamic impedance study of ethanol and acetaldehyde oxidation at platinum in acid solutions, Electrochimica Acta 78 (2012) 286–293. https://doi.org/10.1016/j.electacta.2012.05.102.

[99] S. Yamazaki, T. Ito, M. Yamagata, M. Ishikawa, Non-aqueous electrochemical capacitor utilizing electrolytic redox reactions of bromide species in ionic liquid, Electrochim. Acta 86 (2012) 294–297. https://doi.org/10.1016/j.electacta.2012.01.031.
[100] T. Thomberg, E. Lust, A. Jänes, Iodide ion containing ionic liquid mixture based asymmetrical capacitor performance, J. Energy Storage 32 (2020) 101845. https://doi.org/10.1016/j.est.2020.101845.
[101] J.E.F. Weaver, D. Breadner, F. Deng, B. Ramjee, P.J. Ragogna, R.W. Murray, Electrochemistry of Ferrocene-Functionalized Phosphonium Ionic Liquids, J. Phys. Chem. C 115 (2011) 19379–19385. https://doi.org/10.1021/jp206927w.
[102] G. Sun, K. Li, C. Sun, Electrochemical performance of electrochemical capacitors using Cu(II)-containing ionic liquid as the electrolyte, Microporous and Mesoporous Materials 128 (2010) 56–61. https://doi.org/10.1016/j.micromeso.2009.07.027.
[103] S. Zhang, Z. Bo, H. Yang, J. Yang, L. Duan, J. Yan, K. Cen, Insights into the effects of solvent properties in graphene based electric double-layer capacitors with organic electrolytes, Journal of Power Sources 334 (2016) 162–169. https://doi.org/10.1016/j.jpowsour.2016.10.021.
[104] X. Jin, L. Chen, H. Chen, L. Zhang, W. Wang, H. Ji, S. Deng, L. Jiang, XRD and TEM analyses of a simulated leached rare earth ore deposit: Implications for clay mineral contents and structural evolution, Ecotoxicology and Environmental Safety 225 (2021) 112728. https://doi.org/10.1016/j.ecoenv.2021.112728.
[105] R. Schramm, Use of X-ray Fluorescence Analysis for the Determination of Rare Earth Elements, Physical Sciences Reviews 1 (2016). https://doi.org/10.1515/psr-2016-0061.
[106] M. Černá, E. Volaufová, V. Rod, Extraction of light rare earth elements by amines at high inorganic nitrate concentration, Hydrometallurgy 28 (1992) 339–352. https://doi.org/10.1016/0304-386X(92)90039-3.
[107] J. Zhao, Q. Hu, Y. Li, H. Liu, Efficient separation of vanadium from chromium by a novel ionic liquid-based synergistic extraction strategy, Chemical Engineering Journal 264 (2015) 487–496. https://doi.org/10.1016/j.cej.2014.11.071.
[108] R. Atkin, N. Borisenko, M. Drüschler, F. Endres, R. Hayes, B. Huber, B. Roling, Structure and dynamics of the interfacial layer between ionic liquids and electrode materials, J. Mol. Liq. 192 (2014) 44–54. https://doi.org/10.1016/j.molliq.2013.08.006.
[109] R. Abdallah, A. Derghane, Y.-Y. Lou, O. Merdrignac-Conanec, D. Floner, F. Geneste, New porous bismuth electrode material with high surface area, Journal of Electroanalytical Chemistry 839 (2019) 32–38. https://doi.org/10.1016/j.jelechem.2019.03.023.
[110] P. Bagri, H. Luo, I. Popovs, B.P. Thapaliya, J. Dehaudt, S. Dai, Trimethyl phosphate based neutral ligand room temperature ionic liquids for electrodeposition of rare earth elements, Electrochemistry Communications 96 (2018) 88–92. https://doi.org/10.1016/j.elecom.2018.10.001.
[111] T. Romann, E. Lust, Electrochemical properties of porous bismuth electrodes, Electrochimica Acta 55 (2010) 5746–5752. https://doi.org/10.1016/j.electacta.2010.05.012.

9. SUMMARY IN ESTONIAN

Haruldaste muldmetallide eraldamine fosforiidimaagist kastudes vedelikekstraktsiooni meetodit ning sellele järgnevat elektrokeemilist redutseerimist

Haruldased muldmetallid ja selle ühendid on erinevate omaduste tõttu kaasaegse tehnoloogia jaoks kriitilise tähtsusega materjalid. Kuna nõudlus mõne haruldase muldmetalli elemendi järgi on kasvutrendis, võib tekkida olukord kus pakkumine ei suuda katta nõudlust. Käesoleva doktoritöö eesmärgiks on välja pakkuda uudne moodus haruldaste muldmetallide eraldamiseks Eesti fosforiidimaagist, kasutades esimeses etapis vedelik ekstraktsiooni ning seejärel elektrokeemilist redutseerimist.

Vedelik ekstraktsiooni käigus viiakse omavahel kokku 2 segunematut vedelikku, mille tulemusena mõned elemendid liiguvad läbi piirpinna teise vedeliku faasi. Ekstraktsiooni tingimuste muutmisega on võimalik eraldada huvipakkuvad elemendid ülejäänud materjalist.

Elektrokeemiline sadestamine on meetod, kus kindlad elemendid redutseeritakse elektroodi pinnale. Elektrokeemilise sadestamise tulemusi saab peamiselt mõjutada elektrolüüdi koostise ning rakendatud elektrilise pinge abil.

Käesoleva doktoritöö eesmärkideks on

a) Pakkuda välja parim vedelikekstraktsiooni meetod haruldaste muldmetallide eraldamiseks fosforiidimaagist (I, III)

b) Uurida elektrokeemilise sadestamise mehhanisme juhul kui elektrolüüt sisaldab vaid ühte valitud haruldase muldmetalli soola ning viia läbi selle elemendi elektrokeemiline sadestamine (II)

c) Uurida elektrokeemilise sadestamise mehhanisme juhul kui elektrolüüt sisaldab endas materjali, mis on saadud fosforiidimaagi eelneva puhastamisega vedelik ekstraktsiooni meetodil ning sadestada elektroodile valitud haruldase muldmetalli element. (III)

Uurimistöös kasutati kombineeritud meetodite tulemusi mõõdeti indutseeritud plasmaspektroskoopia (ICP-MS), tsüklilise voltamperomeetria (CV), elektrokeemilise impedantsspektroskoopia (EIS), kronoamperomeetria, energia hajutava röntgenspektroskoopia (EDS), aatomemissioonspektroskoopia (AES) ja skanneeriva elektronmikroskoopia (SEM) abil.

Uurimistöö käigus arendati välja kahe-etapiline vedelikekstraktsiooni meetod, mille käigus eraldati U, Th, Tl ning seejärel haruldased muldmetallid. Ekstrahentidena kasutati oktüülmetüülammooniumnitraati (A336[NO3]) ning bis(2-etüül-

heksüülfosfaati) (D2EHPA). Radioaktiivsete elementide ning haruldaste muldmetallide eraldamise efektiivsus oli D2EHPA kasutamisel ekstrahendina väga kõrge.

Ühe kindla haruldase muldmetalli soola sisaldava elektrolüüdi eksperimendis viidi edukalt läbi Pr sadestamine kuldelektroodile. Olulise tulemusena on toodud välja vismutkatioonide olemasolu tähtsus elektrolüüdis. Tsükliline voltamperomeetria tuvastas kahe katoodse piigi olemasolu mis viitab, et Pr redutseerumise –1,25 V ja –2,6V juures toimub mitmes etapis. Peale 10 tunni pikkust elektrokeemilist sadestamist kronoameromeetria režiimil oli elektrolüüdi lahusest ($Pr(NO_3)_3$ + $Bi(OTf)_3$ + BMPyrrFSI) välja sadenenud ligikaudu 70% esialgsest praseodüümi kogusest.

Uurimistöös eraldati edukalt esialgsest Ülgase fosforiidi kontsentraadi proovist element Y. Peale fosforiidi proovi puhastamist esimeses etapis vedelikekstraktsiooni meetodil sadestati vismutiga modifitseeritud plaatinaelektroodile elemendiline Y (*E*= –2,6V juures)

10. ACKNOWLEDGEMENTS

I would like to express my gratitude to my supervisors Enn Lust and Ove Oll for their great work. Enn, with great knowledge and experience have guided my first steps in electrochemistry. Me and Ove have worked countless hours together to test different theoretical concepts in real conditions. I think we both have learned a lot through the moments of success and failure. Many thanks to both of you for that effort.

I would like especially to thank professor Kalle Kirsimäe, Päärn Paiste, Marianne Külaviir, Peeter Paaver and other nice people from the Department of Geology. They have been my eyes throughout all of these years, providing me with the important results, so I have been able to work in knowledge, not in belief.

I would like to give many thanks to Dr. Karmen Lust for the careful reading of my research articles and this manuscript. Her work has been much more significant than just a careful check of typewriting and style. We have discussed important aspects of physical chemistry which have finally contributed to the quality of this research.

I also would like to thank my other great colleagues in the Department of Chemistry for the moments of interesting discussions and sense of fruitful teamwork. My special thanks belong to Jinfeng for her contributions.

And last but not least, I would like to thank my loving wife Liis for her great support. You have no idea how hard a life with a PhD student might be if you have 5 small children at home. She has carried many times a burden of household management while I was working in the University. Sometimes in the late evenings, sometimes on weekends.

This work was supported by the Estonian Ministry of Education and Research (projects no. IUT 20-13, PUT55, PUT1033 and PUT1107), Education and Youth Board project ÕÜF12 “Extraction of Rare earth elements with ionic liquids” and European Regional Development Fund (Estonian Centre of Excellence TK117T “High-technology Materials for Sustainable Development” and TK141 “Advanced materials and high-technology devices for energy recuperation systems”). This work has also been supported by ASTRA project PER ASPERA Graduate School of Functional Materials and Technologies receiving funding from the European Regional Development Fund under project at University of Tartu, Estonia.

11. PUBLICATIONS

CURRICULUM VITAE

Name: Silvester Jürjo
Date of birth: October 26, 1979
Citizenship: Estonian
Contact: Institute of Chemistry, University of Tartu
Ravila 14A, 50411, Tartu, Estonia
E-mail: silvester.jurjo@ut.ee

Education:

2018–…	University of Tartu, Institute of Chemistry – *Ph.D.* student
2015–2017	Tallinn University of Technology, Institute of Chemistry – *M.Sc.* Applied Chemistry and Biotechnology
2012–2015	Tallinn University of Technology, Insitute of Technology – *B.Sc.* in Materials Science

Professional employment:

2018–…	University of Tartu, Institute of Chemistry, Chemist
2019–…	Chemisty teacher

List of publications:

Jürjo, Silvester; Siinor, Liis; Siimenson, Carolin; Paiste, Päärn; Lust, Enn. Two-Step Solvent Extraction of Radioactive Elements and Rare Earths from Estonian Phosphorite Ore Using Nitrated Aliquat 336 and Bis(2-ethylhexyl) Phosphate. Minerals 2021, 11 (4), 388

Jürjo, Silvester; Oll, Ove; Paiste, Päärn; Külaviir, Marian; Zhao, Jinfeng; Lust, Enn. Electrochemical co-reduction of praseodymium and bismuth from 1-butyl-1-methylpyrrolidinium bis(fluorosulfonyl)imide ionic liquid. Electrochemistry Communications 2022, 138, 107285

Jürjo, Silvester; Oll, Ove; Lust, Enn. Yttrium Separation from Phosphorite Extract Using Liquid Extraction with Room Temperature Ionic Liquids Followed by Electrochemical Reduction. Metals 2024, 14, 927

ELULOOKIRJELDUS

Nimi: Silvester Jürjo
Sünniaeg: 26. oktoober, 1979
Kodakondsus: eesti
Kontakt: Keemiainstituut, Tartu Ülikool
Ravila 14A, 50411, Tartu, Estonia
E-mail: silvester.jurjo@ut.ee

Hariduskäik:

2018–…	Tartu Ülikool, keemiainstituut, doktoriõpe keemia erialal
2015–2017	Tallinna Tehnikaülikool, MSc. rakenduskeemia ja biotehnoloogia erialal
2012–2015	Tallinna Tehnikaülikool, BSc. materjalitehnoloogia erialal

Teenistuskäik:

2018–…	Tartu Ülikool, keemiainstituut, keemik
2019–…	Keemiaõpetaja

Publikatsioonid:

Jürjo, Silvester; Siinor, Liis; Siimenson, Carolin; Paiste, Päärn; Lust, Enn. Two-Step Solvent Extraction of Radioactive Elements and Rare Earths from Estonian Phosphorite Ore Using Nitrated Aliquat 336 and Bis(2-ethylhexyl) Phosphate. Minerals 2021, 11 (4), 388

Jürjo, Silvester; Oll, Ove; Paiste, Päärn; Külaviir, Marian; Zhao, Jinfeng; Lust, Enn. Electrochemical co-reduction of praseodymium and bismuth from 1-butyl-1-methylpyrrolidinium bis(fluorosulfonyl)imide ionic liquid. Electrochemistry Communications 2022, 138, 107285

Jürjo, Silvester; Oll, Ove; Lust, Enn. Yttrium Separation from Phosphorite Extract Using Liquid Extraction with Room Temperature Ionic Liquids Followed by Electrochemical Reduction. Metals 2024, 14, 927

DISSERTATIONES CHIMICAE UNIVERSITATIS TARTUENSIS

1. **Toomas Tamm.** Quantum-chemical simulation of solvent effects. Tartu, 1993, 110 p.
2. **Peeter Burk.** Theoretical study of gas-phase acid-base equilibria. Tartu, 1994, 96 p.
3. **Victor Lobanov.** Quantitative structure-property relationships in large descriptor spaces. Tartu, 1995, 135 p.
4. **Vahur Mäemets.** The ^{17}O and ^{1}H nuclear magnetic resonance study of H_2O in individual solvents and its charged clusters in aqueous solutions of electrolytes. Tartu, 1997, 140 p.
5. **Andrus Metsala.** Microcanonical rate constant in nonequilibrium distribution of vibrational energy and in restricted intramolecular vibrational energy redistribution on the basis of slater's theory of unimolecular reactions. Tartu, 1997, 150 p.
6. **Uko Maran.** Quantum-mechanical study of potential energy surfaces in different environments. Tartu, 1997, 137 p.
7. **Alar Jänes.** Adsorption of organic compounds on antimony, bismuth and cadmium electrodes. Tartu, 1998, 219 p.
8. **Kaido Tammeveski.** Oxygen electroreduction on thin platinum films and the electrochemical detection of superoxide anion. Tartu, 1998, 139 p.
9. **Ivo Leito.** Studies of Brønsted acid-base equilibria in water and non-aqueous media. Tartu, 1998, 101 p.
10. **Jaan Leis.** Conformational dynamics and equilibria in amides. Tartu, 1998, 131 p.
11. **Toonika Rinken.** The modelling of amperometric biosensors based on oxidoreductases. Tartu, 2000, 108 p.
12. **Dmitri Panov.** Partially solvated Grignard reagents. Tartu, 2000, 64 p.
13. **Kaja Orupõld.** Treatment and analysis of phenolic wastewater with microorganisms. Tartu, 2000, 123 p.
14. **Jüri Ivask.** Ion Chromatographic determination of major anions and cations in polar ice core. Tartu, 2000, 85 p.
15. **Lauri Vares.** Stereoselective Synthesis of Tetrahydrofuran and Tetrahydropyran Derivatives by Use of Asymmetric Horner-Wadsworth-Emmons and Ring Closure Reactions. Tartu, 2000, 184 p.
16. **Martin Lepiku.** Kinetic aspects of dopamine D_2 receptor interactions with specific ligands. Tartu, 2000, 81 p.
17. **Katrin Sak.** Some aspects of ligand specificity of P2Y receptors. Tartu, 2000, 106 p.
18. **Vello Pällin.** The role of solvation in the formation of iotsitch complexes. Tartu, 2001, 95 p.
19. **Katrin Kollist.** Interactions between polycyclic aromatic compounds and humic substances. Tartu, 2001, 93 p.

20. **Ivar Koppel.** Quantum chemical study of acidity of strong and superstrong Brønsted acids. Tartu, 2001, 104 p.
21. **Viljar Pihl.** The study of the substituent and solvent effects on the acidity of OH and CH acids. Tartu, 2001, 132 p.
22. **Natalia Palm.** Specification of the minimum, sufficient and significant set of descriptors for general description of solvent effects. Tartu, 2001, 134 p.
23. **Sulev Sild.** QSPR/QSAR approaches for complex molecular systems. Tartu, 2001, 134 p.
24. **Ruslan Petrukhin.** Industrial applications of the quantitative structure-property relationships. Tartu, 2001, 162 p.
25. **Boris V. Rogovoy.** Synthesis of (benzotriazolyl)carboximidamides and their application in relations with *N*- and *S*-nucleophyles. Tartu, 2002, 84 p.
26. **Koit Herodes.** Solvent effects on UV-vis absorption spectra of some solvatochromic substances in binary solvent mixtures: the preferential solvation model. Tartu, 2002, 102 p.
27. **Anti Perkson.** Synthesis and characterisation of nanostructured carbon. Tartu, 2002, 152 p.
28. **Ivari Kaljurand.** Self-consistent acidity scales of neutral and cationic Brønsted acids in acetonitrile and tetrahydrofuran. Tartu, 2003, 108 p.
29. **Karmen Lust.** Adsorption of anions on bismuth single crystal electrodes. Tartu, 2003, 128 p.
30. **Mare Piirsalu.** Substituent, temperature and solvent effects on the alkaline hydrolysis of substituted phenyl and alkyl esters of benzoic acid. Tartu, 2003, 156 p.
31. **Meeri Sassian.** Reactions of partially solvated Grignard reagents. Tartu, 2003, 78 p.
32. **Tarmo Tamm.** Quantum chemical modelling of polypyrrole. Tartu, 2003. 100 p.
33. **Erik Teinemaa.** The environmental fate of the particulate matter and organic pollutants from an oil shale power plant. Tartu, 2003. 102 p.
34. **Jaana Tammiku-Taul.** Quantum chemical study of the properties of Grignard reagents. Tartu, 2003. 120 p.
35. **Andre Lomaka.** Biomedical applications of predictive computational chemistry. Tartu, 2003. 132 p.
36. **Kostyantyn Kirichenko.** Benzotriazole – Mediated Carbon–Carbon Bond Formation. Tartu, 2003. 132 p.
37. **Gunnar Nurk.** Adsorption kinetics of some organic compounds on bismuth single crystal electrodes. Tartu, 2003, 170 p.
38. **Mati Arulepp.** Electrochemical characteristics of porous carbon materials and electrical double layer capacitors. Tartu, 2003, 196 p.
39. **Dan Cornel Fara.** QSPR modeling of complexation and distribution of organic compounds. Tartu, 2004, 126 p.
40. **Riina Mahlapuu.** Signalling of galanin and amyloid precursor protein through adenylate cyclase. Tartu, 2004, 124 p.

41. **Mihkel Kerikmäe.** Some luminescent materials for dosimetric applications and physical research. Tartu, 2004, 143 p.
42. **Jaanus Kruusma.** Determination of some important trace metal ions in human blood. Tartu, 2004, 115 p.
43. **Urmas Johanson.** Investigations of the electrochemical properties of polypyrrole modified electrodes. Tartu, 2004, 91 p.
44. **Kaido Sillar.** Computational study of the acid sites in zeolite ZSM-5. Tartu, 2004, 80 p.
45. **Aldo Oras.** Kinetic aspects of dATPαS interaction with $P2Y_1$ receptor. Tartu, 2004, 75 p.
46. **Erik Mölder.** Measurement of the oxygen mass transfer through the air-water interface. Tartu, 2005, 73 p.
47. **Thomas Thomberg.** The kinetics of electroreduction of peroxodisulfate anion on cadmium (0001) single crystal electrode. Tartu, 2005, 95 p.
48. **Olavi Loog.** Aspects of condensations of carbonyl compounds and their imine analogues. Tartu, 2005, 83 p.
49. **Siim Salmar.** Effect of ultrasound on ester hydrolysis in aqueous ethanol. Tartu, 2006, 73 p.
50. **Ain Uustare.** Modulation of signal transduction of heptahelical receptors by other receptors and G proteins. Tartu, 2006, 121 p.
51. **Sergei Yurchenko.** Determination of some carcinogenic contaminants in food. Tartu, 2006, 143 p.
52. **Kaido Tämm.** QSPR modeling of some properties of organic compounds. Tartu, 2006, 67 p.
53. **Olga Tšubrik.** New methods in the synthesis of multisubstituted hydrazines. Tartu. 2006, 183 p.
54. **Lilli Sooväli.** Spectrophotometric measurements and their uncertainty in chemical analysis and dissociation constant measurements. Tartu, 2006, 125 p.
55. **Eve Koort.** Uncertainty estimation of potentiometrically measured ph and pK_a values. Tartu, 2006, 139 p.
56. **Sergei Kopanchuk.** Regulation of ligand binding to melanocortin receptor subtypes. Tartu, 2006, 119 p.
57. **Silvar Kallip.** Surface structure of some bismuth and antimony single crystal electrodes. Tartu, 2006, 107 p.
58. **Kristjan Saal.** Surface silanization and its application in biomolecule coupling. Tartu, 2006, 77 p.
59. **Tanel Tätte.** High viscosity $Sn(OBu)_4$ oligomeric concentrates and their applications in technology. Tartu, 2006, 91 p.
60. **Dimitar Atanasov Dobchev**. Robust QSAR methods for the prediction of properties from molecular structure. Tartu, 2006, 118 p.
61. **Hannes Hagu**. Impact of ultrasound on hydrophobic interactions in solutions. Tartu, 2007, 81 p.
62. **Rutha Jäger.** Electroreduction of peroxodisulfate anion on bismuth electrodes. Tartu, 2007, 142 p.

63. **Kaido Viht.** Immobilizable bisubstrate-analogue inhibitors of basophilic protein kinases: development and application in biosensors. Tartu, 2007, 88 p.
64. **Eva-Ingrid Rõõm.** Acid-base equilibria in nonpolar media. Tartu, 2007, 156 p.
65. **Sven Tamp.** DFT study of the cesium cation containing complexes relevant to the cesium cation binding by the humic acids. Tartu, 2007, 102 p.
66. **Jaak Nerut.** Electroreduction of hexacyanoferrate(III) anion on Cadmium (0001) single crystal electrode. Tartu, 2007, 180 p.
67. **Lauri Jalukse.** Measurement uncertainty estimation in amperometric dissolved oxygen concentration measurement. Tartu, 2007, 112 p.
68. **Aime Lust.** Charge state of dopants and ordered clusters formation in CaF_2:Mn and CaF_2:Eu luminophors. Tartu, 2007, 100 p.
69. **Iiris Kahn**. Quantitative Structure-Activity Relationships of environmentally relevant properties. Tartu, 2007, 98 p.
70. **Mari Reinik.** Nitrates, nitrites, N-nitrosamines and polycyclic aromatic hydrocarbons in food: analytical methods, occurrence and dietary intake. Tartu, 2007, 172 p.
71. **Heili Kasuk.** Thermodynamic parameters and adsorption kinetics of organic compounds forming the compact adsorption layer at Bi single crystal electrodes. Tartu, 2007, 212 p.
72. **Erki Enkvist.** Synthesis of adenosine-peptide conjugates for biological applications. Tartu, 2007, 114 p.
73. **Svetoslav Hristov Slavov**. Biomedical applications of the QSAR approach. Tartu, 2007, 146 p.
74. **Eneli Härk.** Electroreduction of complex cations on electrochemically polished Bi(*hkl*) single crystal electrodes. Tartu, 2008, 158 p.
75. **Priit Möller.** Electrochemical characteristics of some cathodes for medium temperature solid oxide fuel cells, synthesized by solid state reaction technique. Tartu, 2008, 90 p.
76. **Signe Viggor.** Impact of biochemical parameters of genetically different pseudomonads at the degradation of phenolic compounds. Tartu, 2008, 122 p.
77. **Ave Sarapuu.** Electrochemical reduction of oxygen on quinone-modified carbon electrodes and on thin films of platinum and gold. Tartu, 2008, 134 p.
78. **Agnes Kütt.** Studies of acid-base equilibria in non-aqueous media. Tartu, 2008, 198 p.
79. **Rouvim Kadis.** Evaluation of measurement uncertainty in analytical chemistry: related concepts and some points of misinterpretation. Tartu, 2008, 118 p.
80. **Valter Reedo.** Elaboration of IVB group metal oxide structures and their possible applications. Tartu, 2008, 98 p.
81. **Aleksei Kuznetsov.** Allosteric effects in reactions catalyzed by the cAMP-dependent protein kinase catalytic subunit. Tartu, 2009, 133 p.

82. **Aleksei Bredihhin.** Use of mono- and polyanions in the synthesis of multisubstituted hydrazine derivatives. Tartu, 2009, 105 p.
83. **Anu Ploom.** Quantitative structure-reactivity analysis in organosilicon chemistry. Tartu, 2009, 99 p.
84. **Argo Vonk.** Determination of adenosine A_{2A}- and dopamine D_1 receptor-specific modulation of adenylate cyclase activity in rat striatum. Tartu, 2009, 129 p.
85. **Indrek Kivi.** Synthesis and electrochemical characterization of porous cathode materials for intermediate temperature solid oxide fuel cells. Tartu, 2009, 177 p.
86. **Jaanus Eskusson.** Synthesis and characterisation of diamond-like carbon thin films prepared by pulsed laser deposition method. Tartu, 2009, 117 p.
87. **Marko Lätt.** Carbide derived microporous carbon and electrical double layer capacitors. Tartu, 2009, 107 p.
88. **Vladimir Stepanov.** Slow conformational changes in dopamine transporter interaction with its ligands. Tartu, 2009, 103 p.
89. **Aleksander Trummal.** Computational Study of Structural and Solvent Effects on Acidities of Some Brønsted Acids. Tartu, 2009, 103 p.
90. **Eerold Vellemäe.** Applications of mischmetal in organic synthesis. Tartu, 2009, 93 p.
91. **Sven Parkel.** Ligand binding to 5-HT_{1A} receptors and its regulation by Mg^{2+} and Mn^{2+}. Tartu, 2010, 99 p.
92. **Signe Vahur.** Expanding the possibilities of ATR-FT-IR spectroscopy in determination of inorganic pigments. Tartu, 2010, 184 p.
93. **Tavo Romann**. Preparation and surface modification of bismuth thin film, porous, and microelectrodes. Tartu, 2010, 155 p.
94. **Nadežda Aleksejeva.** Electrocatalytic reduction of oxygen on carbon nanotube-based nanocomposite materials. Tartu, 2010, 147 p.
95. **Marko Kullapere.** Electrochemical properties of glassy carbon, nickel and gold electrodes modified with aryl groups. Tartu, 2010, 233 p.
96. **Liis Siinor.** Adsorption kinetics of ions at Bi single crystal planes from aqueous electrolyte solutions and room-temperature ionic liquids. Tartu, 2010, 101 p.
97. **Angela Vaasa.** Development of fluorescence-based kinetic and binding assays for characterization of protein kinases and their inhibitors. Tartu 2010, 101 p.
98. **Indrek Tulp.** Multivariate analysis of chemical and biological properties. Tartu 2010, 105 p.
99. **Aare Selberg.** Evaluation of environmental quality in Northern Estonia by the analysis of leachate. Tartu 2010, 117 p.
100. **Darja Lavõgina.** Development of protein kinase inhibitors based on adenosine analogue-oligoarginine conjugates. Tartu 2010, 248 p.
101. **Laura Herm.** Biochemistry of dopamine D_2 receptors and its association with motivated behaviour. Tartu 2010, 156 p.

102. **Terje Raudsepp.** Influence of dopant anions on the electrochemical properties of polypyrrole films. Tartu 2010, 112 p.
103. **Margus Marandi.** Electroformation of Polypyrrole Films: *In-situ* AFM and STM Study. Tartu 2011, 116 p.
104. **Kairi Kivirand.** Diamine oxidase-based biosensors: construction and working principles. Tartu, 2011, 140 p.
105. **Anneli Kruve.** Matrix effects in liquid-chromatography electrospray mass-spectrometry. Tartu, 2011, 156 p.
106. **Gary Urb.** Assessment of environmental impact of oil shale fly ash from PF and CFB combustion. Tartu, 2011, 108 p.
107. **Nikita Oskolkov.** A novel strategy for peptide-mediated cellular delivery and induction of endosomal escape. Tartu, 2011, 106 p.
108. **Dana Martin.** The QSPR/QSAR approach for the prediction of properties of fullerene derivatives. Tartu, 2011, 98 p.
109. **Säde Viirlaid.** Novel glutathione analogues and their antioxidant activity. Tartu, 2011, 106 p.
110. **Ülis Sõukand.** Simultaneous adsorption of Cd^{2+}, Ni^{2+}, and Pb^{2+} on peat. Tartu, 2011, 124 p.
111. **Lauri Lipping.** The acidity of strong and superstrong Brønsted acids, an outreach for the "limits of growth": a quantum chemical study. Tartu, 2011, 124 p.
112. **Heisi Kurig.** Electrical double-layer capacitors based on ionic liquids as electrolytes. Tartu, 2011, 146 p.
113. **Marje Kasari.** Bisubstrate luminescent probes, optical sensors and affinity adsorbents for measurement of active protein kinases in biological samples. Tartu, 2012, 126 p.
114. **Kalev Takkis.** Virtual screening of chemical databases for bioactive molecules. Tartu, 2012, 122 p.
115. **Ksenija Kisseljova**. Synthesis of aza-β^3-amino acid containing peptides and kinetic study of their phosphorylation by protein kinase A. Tartu, 2012, 104 p.
116. **Riin Rebane.** Advanced method development strategy for derivatization LC/ESI/MS. Tartu, 2012, 184 p.
117. **Vladislav Ivaništšev.** Double layer structure and adsorption kinetics of ions at metal electrodes in room temperature ionic liquids. Tartu, 2012, 128 p.
118. **Irja Helm.** High accuracy gravimetric Winkler method for determination of dissolved oxygen. Tartu, 2012, 139 p.
119. **Karin Kipper.** Fluoroalcohols as Components of LC-ESI-MS Eluents: Usage and Applications. Tartu, 2012, 164 p.
120. **Arno Ratas.** Energy storage and transfer in dosimetric luminescent materials. Tartu, 2012, 163 p.
121. **Reet Reinart-Okugbeni**. Assay systems for characterisation of subtype-selective binding and functional activity of ligands on dopamine receptors. Tartu, 2012, 159 p.

122. **Lauri Sikk.** Computational study of the Sonogashira cross-coupling reaction. Tartu, 2012, 81 p.
123. **Karita Raudkivi.** Neurochemical studies on inter-individual differences in affect-related behaviour of the laboratory rat. Tartu, 2012, 161 p.
124. **Indrek Saar.** Design of GalR2 subtype specific ligands: their role in depression-like behavior and feeding regulation. Tartu, 2013, 126 p.
125. **Ann Laheäär.** Electrochemical characterization of alkali metal salt based non-aqueous electrolytes for supercapacitors. Tartu, 2013, 127 p.
126. **Kerli Tõnurist.** Influence of electrospun separator materials properties on electrochemical performance of electrical double-layer capacitors. Tartu, 2013, 147 p.
127. **Kaija Põhako-Esko.** Novel organic and inorganic ionogels: preparation and characterization. Tartu, 2013, 124 p.
128. **Ivar Kruusenberg.** Electroreduction of oxygen on carbon nanomaterial-based catalysts. Tartu, 2013, 191 p.
129. **Sander Piiskop.** Kinetic effects of ultrasound in aqueous acetonitrile solutions. Tartu, 2013, 95 p.
130. **Ilona Faustova**. Regulatory role of L-type pyruvate kinase N-terminal domain. Tartu, 2013, 109 p.
131. **Kadi Tamm.** Synthesis and characterization of the micro-mesoporous anode materials and testing of the medium temperature solid oxide fuel cell single cells. Tartu, 2013, 138 p.
132. **Iva Bozhidarova Stoyanova-Slavova.** Validation of QSAR/QSPR for regulatory purposes. Tartu, 2013, 109 p.
133. **Vitali Grozovski**. Adsorption of organic molecules at single crystal electrodes studied by *in situ* STM method. Tartu, 2014, 146 p.
134. **Santa Veikšina**. Development of assay systems for characterisation of ligand binding properties to melanocortin 4 receptors. Tartu, 2014, 151 p.
135. **Jüri Liiv.** PVDF (polyvinylidene difluoride) as material for active element of twisting-ball displays. Tartu, 2014, 111 p.
136. **Kersti Vaarmets.** Electrochemical and physical characterization of pristine and activated molybdenum carbide-derived carbon electrodes for the oxygen electroreduction reaction. Tartu, 2014, 131 p.
137. **Lauri Tõntson**. Regulation of G-protein subtypes by receptors, guanine nucleotides and Mn^{2+}. Tartu, 2014, 105 p.
138. **Aiko Adamson.** Properties of amine-boranes and phosphorus analogues in the gas phase. Tartu, 2014, 78 p.
139. **Elo Kibena**. Electrochemical grafting of glassy carbon, gold, highly oriented pyrolytic graphite and chemical vapour deposition-grown graphene electrodes by diazonium reduction method. Tartu, 2014, 184 p.
140. **Teemu Näykki.** Novel Tools for Water Quality Monitoring – From Field to Laboratory. Tartu, 2014, 202 p.
141. **Karl Kaupmees.** Acidity and basicity in non-aqueous media: importance of solvent properties and purity. Tartu, 2014, 128 p.

142. **Oleg Lebedev**. Hydrazine polyanions: different strategies in the synthesis of heterocycles. Tartu, 2015, 118 p.
143. **Geven Piir.** Environmental risk assessment of chemicals using QSAR methods. Tartu, 2015, 123 p.
144. **Olga Mazina.** Development and application of the biosensor assay for measurements of cyclic adenosine monophosphate in studies of G protein-coupled receptor signalinga. Tartu, 2015, 116 p.
145. **Sandip Ashokrao Kadam.** Anion receptors: synthesis and accurate binding measurements. Tartu, 2015, 116 p.
146. **Indrek Tallo.** Synthesis and characterization of new micro-mesoporous carbide derived carbon materials for high energy and power density electrical double layer capacitors. Tartu, 2015, 148 p.
147. **Heiki Erikson.** Electrochemical reduction of oxygen on nanostructured palladium and gold catalysts. Tartu, 2015, 204 p.
148. **Erik Anderson.** *In situ* Scanning Tunnelling Microscopy studies of the interfacial structure between Bi(111) electrode and a room temperature ionic liquid. Tartu, 2015, 118 p.
149. **Girinath G. Pillai.** Computational Modelling of Diverse Chemical, Biochemical and Biomedical Properties. Tartu, 2015, 140 p.
150. **Piret Pikma.** Interfacial structure and adsorption of organic compounds at Cd(0001) and Sb(111) electrodes from ionic liquid and aqueous electrolytes: an *in situ* STM study. Tartu, 2015, 126 p.
151. **Ganesh babu Manoharan.** Combining chemical and genetic approaches for photoluminescence assays of protein kinases. Tartu, 2016, 126 p.
152. **Carolin Siimenson**. Electrochemical characterization of halide ion adsorption from liquid mixtures at Bi(111) and pyrolytic graphite electrode surface. Tartu, 2016, 110 p.
153. **Asko Laaniste.** Comparison and optimisation of novel mass spectrometry ionisation sources. Tartu, 2016, 156 p.
154. **Hanno Evard.** Estimating limit of detection for mass spectrometric analysis methods. Tartu, 2016, 224 p.
155. **Kadri Ligi.** Characterization and application of protein kinase-responsive organic probes with triplet-singlet energy transfer. Tartu, 2016, 122 p.
156. **Margarita Kagan.** Biosensing penicillins' residues in milk flows. Tartu, 2016, 130 p.
157. **Marie Kriisa.** Development of protein kinase-responsive photoluminescent probes and cellular regulators of protein phosphorylation. Tartu, 2016, 106 p.
158. **Mihkel Vestli.** Ultrasonic spray pyrolysis deposited electrolyte layers for intermediate temperature solid oxide fuel cells. Tartu, 2016, 156 p.
159. **Silver Sepp**. Influence of porosity of the carbide-derived carbon on the properties of the composite electrocatalysts and characteristics of polymer electrolyte fuel cells. Tartu, 2016, 137 p.
160. **Kristjan Haav**. Quantitative relative equilibrium constant measurements in supramolecular chemistry. Tartu, 2017, 158 p.

161. **Anu Teearu**. Development of MALDI-FT-ICR-MS methodology for the analysis of resinous materials. Tartu, 2017, 205 p.
162. **Taavi Ivan**. Bifunctional inhibitors and photoluminescent probes for studies on protein complexes. Tartu, 2017, 140 p.
163. **Maarja-Liisa Oldekop**. Characterization of amino acid derivatization reagents for LC-MS analysis. Tartu, 2017, 147 p.
164. **Kristel Jukk**. Electrochemical reduction of oxygen on platinum- and palladium-based nanocatalysts. Tartu, 2017, 250 p.
165. **Siim Kukk**. Kinetic aspects of interaction between dopamine transporter and *N*-substituted nortropane derivatives. Tartu, 2017, 107 p.
166. **Birgit Viira**. Design and modelling in early drug development in targeting HIV-1 reverse transcriptase and Malaria. Tartu, 2017, 172 p.
167. **Rait Kivi**. Allostery in cAMP dependent protein kinase catalytic subunit. Tartu, 2017, 115 p.
168. **Agnes Heering**. Experimental realization and applications of the unified acidity scale. Tartu, 2017, 123 p.
169. **Delia Juronen**. Biosensing system for the rapid multiplex detection of mastitis-causing pathogens in milk. Tartu, 2018, 85 p.
170. **Hedi Rahnel.** ARC-inhibitors: from reliable biochemical assays to regulators of physiology of cells. Tartu, 2018, 176 p.
171. **Anton Ruzanov.** Computational investigation of the electrical double layer at metal–aqueous solution and metal–ionic liquid interfaces. Tartu, 2018, 129 p.
172. **Katrin Kestav.** Crystal Structure-Guided Development of Bisubstrate-Analogue Inhibitors of Mitotic Protein Kinase Haspin. Tartu, 2018, 166 p.
173. **Mihkel Ilisson.** Synthesis of novel heterocyclic hydrazine derivatives and their conjugates. Tartu, 2018, 101 p.
174. **Anni Allikalt.** Development of assay systems for studying ligand binding to dopamine receptors. Tartu, 2018, 160 p.
175. **Ove Oll.** Electrical double layer structure and energy storage characteristics of ionic liquid based capacitors. Tartu, 2018, 187 p.
176. **Rasmus Palm.** Carbon materials for energy storage applications. Tartu, 2018, 114 p.
177. **Jörgen Metsik.** Preparation and stability of poly(3,4-ethylenedioxythiophene) thin films for transparent electrode applications. Tartu, 2018, 111 p.
178. **Sofja Tšepelevitš.** Experimental studies and modeling of solute-solvent interactions. Tartu, 2018, 109 p.
179. **Märt Lõkov.** Basicity of some nitrogen, phosphorus and carbon bases in acetonitrile. Tartu, 2018, 104 p.
180. **Anton Mastitski**. Preparation of α-aza-amino acid precursors and related compounds by novel methods of reductive one-pot alkylation and direct alkylation. Tartu, 2018, 155 p.
181. **Jürgen Vahter**. Development of bisubstrate inhibitors for protein kinase CK2. Tartu, 2019, 186 p.

182. **Piia Liigand.** Expanding and improving methodology and applications of ionization efficiency measurements. Tartu, 2019, 189 p.
183. **Sigrid Selberg.** Synthesis and properties of lipophilic phosphazene-based indicator molecules. Tartu, 2019, 74 p.
184. **Jaanus Liigand.** Standard substance free quantification for LC/ESI/MS analysis based on the predicted ionization efficiencies. Tartu, 2019, 254 p.
185. **Marek Mooste.** Surface and electrochemical characterisation of aryl film and nanocomposite material modified carbon and metal-based electrodes. Tartu, 2019, 304 p.
186. **Mare Oja.** Experimental investigation and modelling of pH profiles for effective membrane permeability of drug substances. Tartu, 2019, 306 p.
187. **Sajid Hussain.** Electrochemical reduction of oxygen on supported Pt catalysts. Tartu, 2019, 220 p.
188. **Ronald Väli.** Glucose-derived hard carbon electrode materials for sodium-ion batteries. Tartu, 2019, 180 p.
189. **Ester Tee.** Analysis and development of selective synthesis methods of hierarchical micro- and mesoporous carbons. Tartu, 2019, 210 p.
190. **Martin Maide.** Influence of the microstructure and chemical composition of the fuel electrode on the electrochemical performance of reversible solid oxide fuel cell. Tartu, 2020, 144 p.
191. **Edith Viirlaid.** Biosensing Pesticides in Water Samples. Tartu, 2020, 102 p.
192. **Maike Käärik.** Nanoporous carbon: the controlled nanostructure, and structure-property relationships. Tartu, 2020, 162 p.
193. **Artur Gornischeff.** Study of ionization efficiencies for derivatized compounds in LC/ESI/MS and their application for targeted analysis. Tartu, 2020, 124 p.
194. **Reet Link.** Ligand binding, allosteric modulation and constitutive activity of melanocortin-4 receptors. Tartu, 2020, 108 p.
195. **Pilleriin Peets.** Development of instrumental methods for the analysis of textile fibres and dyes. Tartu, 2020, 150 p.
196. **Larisa Ivanova.** Design of active compounds against neurodegenerative diseases. Tartu, 2020, 152 p.
197. **Meelis Härmas.** Impact of activated carbon microstructure and porosity on electrochemical performance of electrical double-layer capacitors. Tartu, 2020, 122 p.
198. **Ruta Hecht.** Novel Eluent Additives for LC-MS Based Bioanalytical Methods. Tartu, 2020, 202 p.
199. **Max Hecht.** Advances in the Development of a Point-of-Care Mass Spectrometer Test. Tartu, 2020, 168 p.
200. **Ida Rahu.** Bromine formation in inorganic bromide/nitrate mixtures and its application for oxidative aromatic bromination. Tartu, 2020, 116 p.
201. **Sander Ratso**. Electrocatalysis of oxygen reduction on non-precious metal catalysts. Tartu, 2020, 371 p.
202. **Astrid Darnell.** Computational design of anion receptors and evaluation of host-guest binding. Tartu, 2021, 150 p.

203. **Ove Korjus.** The development of ceramic fuel electrode for solid oxide cells. Tartu, 2021, 150 p.
204. **Merit Oss.** Ionization efficiency in electrospray ionization source and its relations to compounds' physico-chemical properties. Tartu, 2021, 124 p.
205. **Madis Lüsi**. Electroreduction of oxygen on nanostructured palladium catalysts. Tartu, 2021, 180 p.
206. **Eliise Tammekivi.** Derivatization and quantitative gas-chromatographic analysis of oils. Tartu, 2021, 122 p.
207. **Simona Selberg.** Development of Small-Molecule Regulators of Epi-transcriptomic Processes. Tartu, 2021, 122 p.
208. **Olivier Etebe Nonga.** Inhibitors and photoluminescent probes for in vitro studies on protein kinases PKA and PIM. Tartu, 2021, 189 p.
209. **Riinu Härmas.** The structure and H2 diffusion in porous carbide-derived carbon particles. Tartu, 2022, 123 p.
210. **Maarja Paalo.** Synthesis and characterization of novel carbon electrodes for high power density electrochemical capacitors. Tartu, 2022, 144 p.
211. **Jinfeng Zhao.** Electrochemical characteristics of Bi(hkl) and micro-meso-porous carbon electrodes in ionic liquid based electrolytes. Tartu, 2022, 134 p.
212. **Alar Heinsaar.** Investigation of oxygen electrode materials for high-temperature solid oxide cells in natural conditions. Tartu, 2022, 120 p.
213. **Jaana Lilloja.** Transition metal and nitrogen doped nanocarbon cathode catalysts for anion exchange membrane fuel cells. Tartu, 2022, 202 p.
214. **Maris-Johanna Tahk.** Novel fluorescence-based methods for illuminating transmembrane signal transduction by G-protein coupled receptors. Tartu, 2022, 200 p.
215. **Eerik Jõgi.** Development and Applications of E. coli Immunosensor. Tartu, 2022, 103 p.
216. **Alo Rüütel.** Design principles of synthetic molecular receptors for anion-selective electrodes. Tartu, 2022, 109 p.
217. **Tanel Sõrmus.** Development of stimuli-responsive and covalent bisub-strate inhibitors of protein kinases. Tartu, 2022, 148 p.
218. **Oleg Artemchuk.** Autotrophic nitrogen removal processes for nutrient removal from sidestream and mainstream wastewater. Tartu, 2022, 115 p.
219. **Andre Leesment.** Quantitative studies of Brønsted acidity in biphasic systems and gas-phase. Tartu, 2023, 83 p.
220. **Meeli Arujõe-Sado.** Structural effects in aza-peptide bond formation re-action. Tartu, 2023, 83 p.
221. **Jonas Mart Linge.** Electrochemical reduction of oxygen on silver-based catalysts. Tartu, 2023, 269 p.
222. **Tõnis Laasfeld.** Integrating Image Analysis and Quantitative Modeling for a Holistic View of GPCR Ligand Binding Dynamics. Tartu, 2023, 226 p.
223. **Ernesto de Jesus Zapata Flores.** Derivatization Reagents used in nega-tive mode electrospray LC-MS. Tartu, 2023, 107 p.

224. **Patrick Teppor.** Obtaining platinum-free oxygen reduction catalysts through biomass valorization: a case study of peat. Tartu, 2023, 161 p.
225. **Peeter Valk.** Methanol Oxidation on Platinum-Rare-Earth Metal Oxide Activated Catalysts. Tartu, 2023, 162 p.
226. **Shidong Chen.** Unravelling prehistoric plant exploitation in eastern Baltic: organic residue analysis of plant-based materials by multi-method approach. Tartu, 2023, 245 p.
227. **Yogesh Kumar.** M-N_4 macrocycle-based catalysts for electrocatalysis of oxygen reduction and oxygen evolution. Tartu, 2023, 224 p.
228. **Kerli Martin.** Recognition of carboxylates by synthetic receptors – from structure-affinity studies to solid-contact anion-selective electrode prototyping. Tartu, 2024, 130 p.
229. **Huy Quí Vinh Nguyen.** Development of Carbon Supported Pt–CeO_2 Catalysts for Proton Exchange Membrane Fuel Cells. Tartu, 2024, 198 p.
230. **Heigo Ers**. Adsorption and Structuring Processes at Single Crystal Electrode – Ionic Liquid Interface – Insights from Simulations and *in situ* Studies. Tartu, 2024, 137 p.
231. **Ritums Cepitis.** Modelling Structural and Geometrical Effects in Carbon Dioxide and Oxygen Electrocatalysis. Tartu, 2024, 99 p.
232. **Kaarel Kisand.** Resorcinol-derived carbon-based catalysts for polymer electrolyte fuel cell cathodes. Tartu, 2024, 205 p.
233. **Akmal Kosimov**. Template-assisted Mechanosynthesis (TAMS) for the production of bifunctional transition metal-based catalysts. Tartu, 2024, 123 p.
234. **Larissa Silva Macieli.** Derivatization-targeted LC-MS analysis of compounds containing amino group. Tartu, 2024, 157 p.